HDL

HDL-PR-77-2—*Status of the Tactical Environment Multiple Systems Evaluation Program (TEMSEP)*, by John N. Bombardt, Jr., John F. W. Dietz, George Merkel, and Daniel J. Spohn

Status of the Tactical Environment Multiple Systems Evaluation Program (TEMSEP)

October 1977

This work was sponsored in part by the Defense Nuclear Agency
under subtask R99QAXEB088, EMP Interaction and Coupling Phenomenology.

RESEARCH
DEVELOPMENT
ENGINEERING

U.S. Army Materiel Development
and Readiness Command
HARRY DIAMOND LABORATORIES
Adelphi, Maryland 20783

UNCLASSIFIED

SECURITY CLASSIFICATION OF THIS PAGE (When Data Entered)

REPORT DOCUMENTATION PAGE

READ INSTRUCTIONS BEFORE COMPLETING FORM

1. REPORT NUMBER: HDL-PR-77-2
2. GOVT ACCESSION NO.:
3. RECIPIENT'S CATALOG NUMBER:
4. TITLE (and Subtitle): Status of the Tactical Environment Multiple Systems Evaluation Program (TEMSEP)
5. TYPE OF REPORT & PERIOD COVERED: Progress Report
6. PERFORMING ORG. REPORT NUMBER:
7. AUTHOR(s): John N. Bombardt, Jr.; John F. W. Dietz; George Merkel; Daniel J. Spohn
8. CONTRACT OR GRANT NUMBER(s): DA: 1L1621188AH75
9. PERFORMING ORGANIZATION NAME AND ADDRESS: Harry Diamond Laboratories, 2800 Powder Mill Road, Adelphi, MD 20783
10. PROGRAM ELEMENT, PROJECT, TASK AREA & WORK UNIT NUMBERS: Program Ele. 6.27.04.H; Program Ele. 6.21.18.A
11. CONTROLLING OFFICE NAME AND ADDRESS: Defense Nuclear Agency, Washington, DC 20305
12. REPORT DATE: October 1977
13. NUMBER OF PAGES: 55
14. CONTROLLING OFFICE NAME AND ADDRESS: US Army Materiel Development & Readiness Command, 5001 Eisenhower Avenue, Alexandria, VA 22333
15. SECURITY CLASS. (of this report): Unclassified
15a. DECLASSIFICATION/DOWNGRADING SCHEDULE:
16. DISTRIBUTION STATEMENT (of this Report): Approved for public release; distribution unlimited.
17. DISTRIBUTION STATEMENT (of the abstract entered in Block 20, if different from Report):
18. SUPPLEMENTARY NOTES:
    DRCMS Code: 36AA.7210062704
    DRCMS Code: 612118.H750011
    HDL Project: E057E3
    HDL Project: X757E7
    This work was sponsored in part by the Defense Nuclear Agency under subtask R99QAXEB088, EMP Interaction and Coupling Phenomenology.
19. KEY WORDS (Continue on reverse side if necessary and identify by block number):
    EMP
    Tactical nuclear threats
    Simulation
    Flash x ray
20. ABSTRACT (Continue on reverse side if necessary and identify by block number)

This report discusses technical progress made during FY76 under the Defense Nuclear Agency (DNA) sponsored Tactical Environment Multiple Systems Evaluation Program (TEMSEP). The long and short range goals of the program are presented with particular emphasis on the topics of instrumentation in an ionizing radiation environment, basic phenomena associated with the electromagnetic pulse (EMP) generation within the nuclear source region, and

laboratory simulation of the electromagnetic environment associated with the nearby (endoatmospheric) detonation of a nuclear weapon. Experiments used the AURORA Flash X-Ray Facility as a radiation source. Notable milestones accomplished during FY76 were the experimental verification of the existence of the "boundary layer" phenomenon and verification of electromagnetic coupling models for simple structures.

FOREWORD

The work reported here was sponsored primarily by the Defense Nuclear Agency (DNA) under subtask R99QAXEB088. The authors acknowledge the guidance and contributions of two DNA Project Officers: William Adams in the early stages of program formulation and W. D. Wilson in insuring program continuity during 1976. Also, we are appreciative of help received from Paul Caldwell and his staff at the Harry Diamond Laboratories AURORA Flash X-Ray Facility; in particular, we thank Stewart Graybill, Klaus Kerris, and Denis Whittaker for their contributions during our AURORA experiments. Within our own organization, Laboratory 1000, Robert Pfeffer managed the work during much of FY76 and Leedy Ambrose and Joseph Capobianco provided us with valuable experimental assistance. Finally, we take this opportunity to express our thanks to Jean Ciccarelli for preparation of the original manuscript.

CONTENTS

FIGURES

FIGURES (Cont'd)

TABLE

1. PROGRAMMATIC OVERVIEW

1.1 Objectives and Scope

The Tactical Environment Multiple Systems Evaluation Program (TEMSEP) is jointly funded at the Harry Diamond Laboratories (HDL) by the Army and the Defense Nuclear Agency (DNA) and is directed toward vulnerability assessments and hardening of tactical military equipment for tactical nuclear threats. Specifically, the ultimate goals of TEMSEP are these:

a. Develop methods to assess by analysis and experimentation the electromagnetic pulse (EMP) vulnerabilities of military equipment for endoatmospheric nuclear threats

b. Predict EMP vulnerabilities of critical military equipment to endoatmospheric nuclear threats

c. Determine the relative effects on critical military equipment of endoatmospheric and exoatmospheric nuclear threats

d. Evaluate the effectiveness of EMP hardening measures associated with exoatmospheric nuclear threats for protection against endoatmospheric nuclear threats

e. Recommend appropriate EMP hardening measures to insure system survivability in a tactical nuclear environment.

In general, the DNA-sponsored portion of TEMSEP addresses the following matters: (1) the definition of EMP environmental criteria for tactical scenarios, (2) the development of interaction and coupling technology for critical tactical systems in the intermediate region of "weak" Compton currents, and (3) the evaluation of the feasibility of simulating tactical source-region EMP environments by using the HDL AURORA Flash X-Ray Facility. The Army-sponsored portion of TEMSEP, on the other hand, is concerned with vulnerability assessments and hardening recommendations for actual Army equipment.

The purpose of this report is to review TEMSEP and the progress made in this program during FY76, with the primary emphasis on the applied research which was sponsored by DNA. Interaction and coupling studies, damage analyses, and vulnerability assessments of the Lance Missile System and the AN/GRC-106 Radio System were performed in TEMSEP during FY76 under sponsorship of the Army; this Army-sponsored work is not discussed at length in this report. Some of the DNA-sponsored work done in TEMSEP during FY76 has been reported in the open literature.[1]

[1]*J. F. W. Dietz, G. Merkel, and D. Spohn, Radiation Induced Coupling to a Truncated Cylinder within a Cylinder, IEEE Trans. Nucl. Sci.,* *__NS-23__* *(December 1976).*

1.2 Approach

The total programmatic approach of TEMSEP, is as follows:

a. From the defense intelligence community and related EMP vulnerability assessment and hardening programs (such as the Multiple Systems Evaluation Program[1]), identify critical foreign and domestic tactical systems.

b. Define the characteristics of these equipments which contribute to their susceptibility to tactical nuclear threats.

c. Develop the interaction and coupling technology necessary to analyze such characteristics and to determine system vulnerability.

d. Develop the experimental and theoretical techniques necessary to evaluate system susceptibility on the terminal and circuit level.

e. Establish susceptibilities and assess vulnerabilities of a tractable set of critical foreign and domestic systems involved in tactical scenarios.

f. Evaluate the effectiveness of conventional hardening measures (such as filtering, terminal protection, and isolation) for tactical EMP threats, and develop generic hardening measures applicable to many subsystems of the same general type.

g. Identify research requirements (such as interaction and coupling phenomena, circuit and damage models, and device development for terminal and circuit protection) resulting from the technology voids which impede meaningful vulnerability assessment and hardening of critical domestic systems.

A key step in the above programmatic approach is the development of the interaction and coupling technology necessary to assess system vulnerability. This step involves not only the development of experimental and theoretical techniques for predicting and evaluating responses of dominant interaction and coupling mechanisms (as these appear in actual systems), but also the conception and experimental verification of technically feasible schemes for simulating tactical source-region EMP environments. With regard to the latter, no existing threat-relatable EMP simulator can produce all of the electromagnetic characteristics of a tactical near-surface nuclear detonation, including the proper electromagnetic field components, time-varying air conductivity, and Compton current. In addition, no data gathered during atmospheric tests or during recent underground tests are pertinent (with respect to both the time and the dose) to the

[1] *J. F. W. Dietz, G. Merkel, and D. Spohn, Radiation Induced Coupling to a Truncated Cylinder within a Cylinder, IEEE Trans. Nucl. Sci., NS-23 (December 1976).*

tactical source region, as shown in figure 1. Nevertheless, intelligent use of flash x-ray machines (in particular, the AURORA Facility) can yield meaningful information that can be used to validate theory or guide the development of theoretical source-region coupling models. In addition, augmentation of the AURORA environment may be possible to simulate a tactical source-region EMP environment which is appropriate for certain types of critical systems.

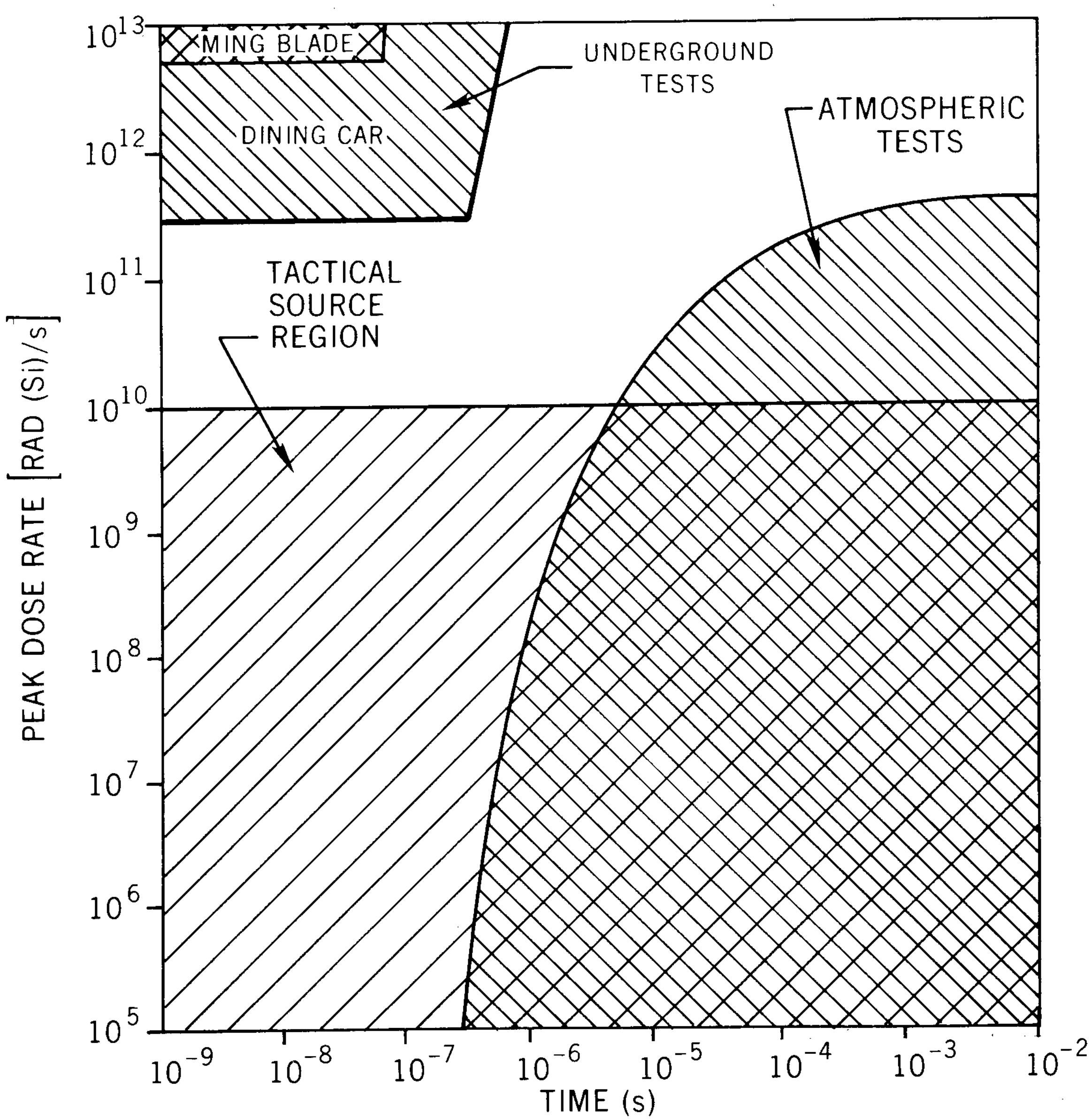

Figure 1. Regions of valid atmospheric test data and recent underground test data (according to R. Shaffer of R and D Associates) and region of interest for tactical source region related research.

Thus, several areas of experimental investigation are important to programmatic success, each of which is designed to contribute to the eventual ability to adequately assess the vulnerability of military equipment to the tactical nuclear threat. These areas are the following:

a. the development of instrumentation for making electromagnetic measurements in the presence of ionizing radiation

b. controlled diagnostic experiments designed to validate or guide theoretical developments (by using the AURORA Facility, the High Intensity Flash X-Ray Facility (HIFX), or both)

c. Comprehensive experimental characterization of the AURORA environment with respect to the gamma source, the electromagnetic field, air conductivity, and Compton current

d. Proof-of-principle experiments designed to evaluate the technical feasibility of simulation concepts involving the AURORA Facility

Although most of HDL's technical effort expended for DNA in FY76 was connected with the areas of experimental investigation listed above, the development of theoretical techniques for predicting and evaluating responses of dominant interaction and coupling mechanisms also received a good deal of attention in FY76 and figures prominently in TEMSEP. The areas of theoretical investigation that presently appear to be of particular programmatic significance are these:

a. The relative importance of electromagnetic excitation (the electromagnetic field and transient air conductivity in the absence of the system) and direct excitation (gamma and Compton-electron) of systems subjected to tactical nuclear threats

b. Evaluation and improvement of state-of-the-art numerical tools for tactical applications

c. Evaluation and improvement of time-phase (particularly, quasi-static) analytical and numerical tools for tactical applications.

The first area of theoretical investigation is concerned with the significance of detailed Monte Carlo sources, self-consistency, and charge-depletion (boundary) layers in a tactical context. The last two areas of theoretical investigation are concerned with establishing the adequacy of existing theoretical techniques and improving them for tactical applications.

2. PROGRAMMATIC MILESTONES

During FY76, several programmatic milestones were identified. These included the successful completion of two AURORA runs (December and March), the awarding of several supporting contracts, the completion of system coupling analyses (Lance and the AN/GRC-106), the running of a new environment code (NEMP), and the identification of potential problem areas (Mission Research Corp. (MRC)/AURORA memorandums and boundary layer reports). Each milestone by itself does not represent a technical accomplishment, but rather is an identifiable effort which is important only in an overall programmatic context. The technical milestones represent the true technical progress made in this program.

2.1 December Test

During early December 1975, a series of experiments was conducted at the AURORA Facility with the primary purpose of determining the adequacy of new instruments which had been designed to function in the radiation environment. In addition, coupling experiments and AURORA gamma-source measurements were carried out. With respect to the four general areas of research addressed in FY76 (coupling, instrumentation, basic phenomena, and simulation), the experiments addressed three of them (coupling, instrumentation, and simulation).

New instrumentation, constructed for use in the March 1976 test, was checked out in the radiation environment. This included a cathode follower, to be used in connection with a Tektronix voltage probe to make high-impedance voltage measurements, and a Compton diode and a collimated Rogowski coil, to be used to measure the Compton current in the air. Response measurements of a concentric box geometry also were made with the intention of being used for comparisons with theory. In simulation, a series of collimated dosimeter measurements was performed to provide information useful for characterizing the AURORA source.

The Compton diode constructed for this test (fig. 2) consisted of an aluminum cylinder 15 cm in diameter with a tungsten collector 6.3 cm in diameter. To collimate the current driving the sensor, Pb (10 cm thick) was used.

The collimated Rogowski coil comprised an Adams Electronic Corp. (ADELCO) current probe (of radius 1.27 cm) collimated with 10 cm of Pb. The probe and Pb were placed in an aluminum cylinder for convenience.

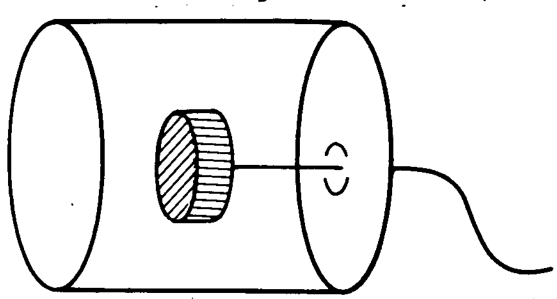

Figure 2. Compton diode.

A cathode follower circuit was constructed to be used as an impedance matching network to drive the low-impedance cable from a high-impedance source while maintaining minimal signal loss (fig. 3). The device was used with a Tektronix P6003 probe to measure the voltage buildup on the center box of the concentric box test geometry used in coupling experiments. The voltage probe was exposed to the unattenuated AURORA radiation within the test geometry, but the cathode follower was provided shielding by being placed inside the center of a stack of Pb bricks. In this configuration, the cathode follower was exposed to a total dose of approximately 5 rads (Si) (3×10^7 rads (Si)/s peak).

Coupling experiments used the basic concentric box geometry shown in figure 4. It consisted of a box 15.24 cm to a side constructed of 0.63-cm aluminum, suspended on nylon rope in a 66-cm square conducting upper chamber of a two-chamber radio frequency interference (RFI) shielded box. The inner aluminum box, located in the center of the upper chamber, was connected with a thin wire to a BNC feed-through cable to the lower chamber where the cathode followers were located. The two chambers were separated by a 2.54-cm-thick aluminum partition. The suspended aluminum box was used in two modes: one with the box empty so that it was thin with respect to the absorption of gamma radiation and another with the box filled with Pb so that it was thick with respect to gamma radiation. The shielded box was symmetrically placed in the AURORA test cell, elevated so that the center of the upper chamber (and the suspended inner aluminum box) was on the axis of the AURORA radiation. In this configuration, the front was exposed to a total dose of approximately 700 rads (Si). The "open-circuit" voltage and short-circuit current were measured on the inner box. In addition, Rogowski coils (to measure the Compton current) and Moebius loops (to measure the magnetic field) were placed at various locations within the upper chamber.

Although it may sometimes be assumed so, the AURORA Facility's "hot spot" is not a point source of radiation. A more reasonable assumption is that it is a disk source of some effective area. To determine this area, an experiment was designed by using thermoluminescent dosimeters (TLD's) placed in holes drilled through various thicknesses of Pb bricks. By measuring the dose and dose rates at the same distance from the source with 0, 5.08, and 10.16 cm of collimation, the effective area of the source can be calculated directly by geometrical considerations.

Data obtained during the December test contributed to some of the significant conclusions that were drawn based on the consideration of the total FY76 effort. Notable examples are the decision to abandon the Compton diode for AURORA application and efforts to continue to develop a high-impedance voltage measurement method. Also, this test impacted plans for the March test by indicating the need for more shielding around the cathode follower and the need for a better method of measuring the Compton current.

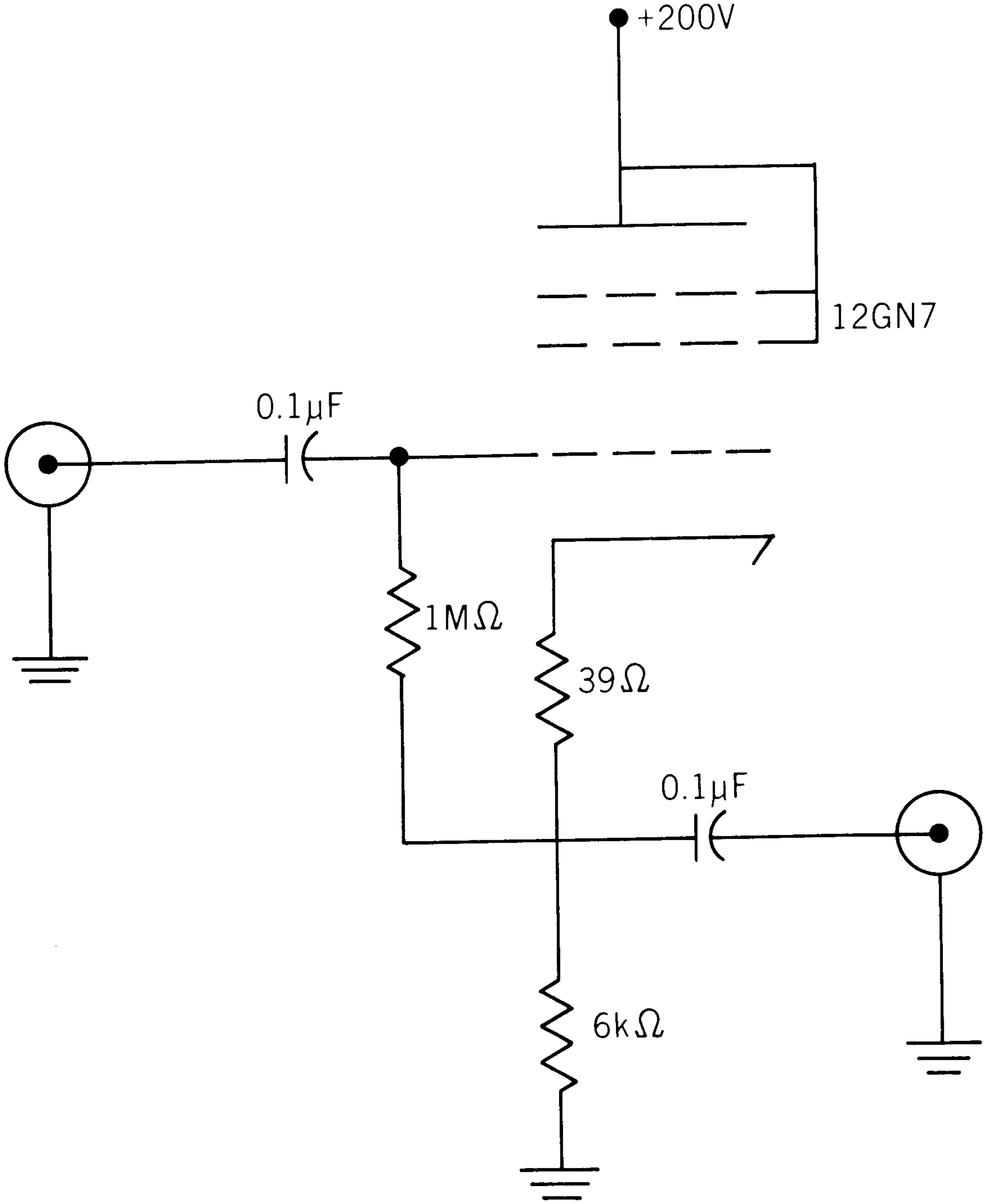

Figure 3. Cathode follower.

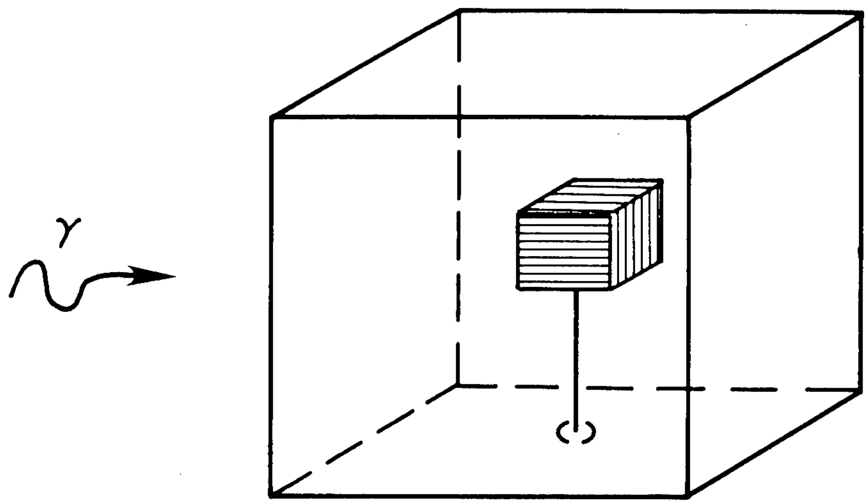

Figure 4. Concentric box test geometry.

2.2 March Test

During March and April 1976, a series of tests was conducted at the AURORA Facility to experimentally investigate several matters concerning the electromagnetic environment generated within the tactical source region. These tests provided information within all four general research areas: coupling, instrumentation, basic phenomena, and simulation. In the coupling area, a series of measurements was made to determine current and voltage responses of simple structures exposed to ionizing radiation. In the instrumentation area, data were obtained from instruments designed to measure Compton current, electric (E-) field, and voltage. In the basic phenomena area, air chemistry was addressed by measuring the effect of the charge-depletion boundary layer. Finally, the feasibility of certain simulation schemes was investigated by considering the charging of gamma-thick objects in the radiation environment and the resulting E-field.

The concentric-cylinder geometry in figure 5 was exposed to the AURORA radiation pulse, and the currents and fields in the medium between the cylinders were measured at various locations. Also, the current on the inner cylinder was measured by splitting the cylinder and connecting the sections with parallel resistors, forcing the axial current to be shared by the resistors. The current through one of the resistors was measured and, from that, the total axial current flowing on the inner cylinder could be inferred.

The validity of this inference was demonstrated via laboratory bench tests in which the inner cylinder was driven with a current source as shown in figure 6. The total current was monitored between the pulser and the inner cylinder (location A), and so was the partitioned current flowing in each of the parallel resistors inserted in the inner

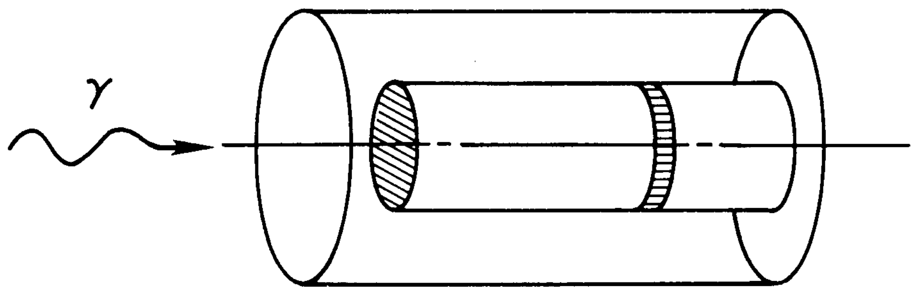

Figure 5. Concentric cylinder test geometry.

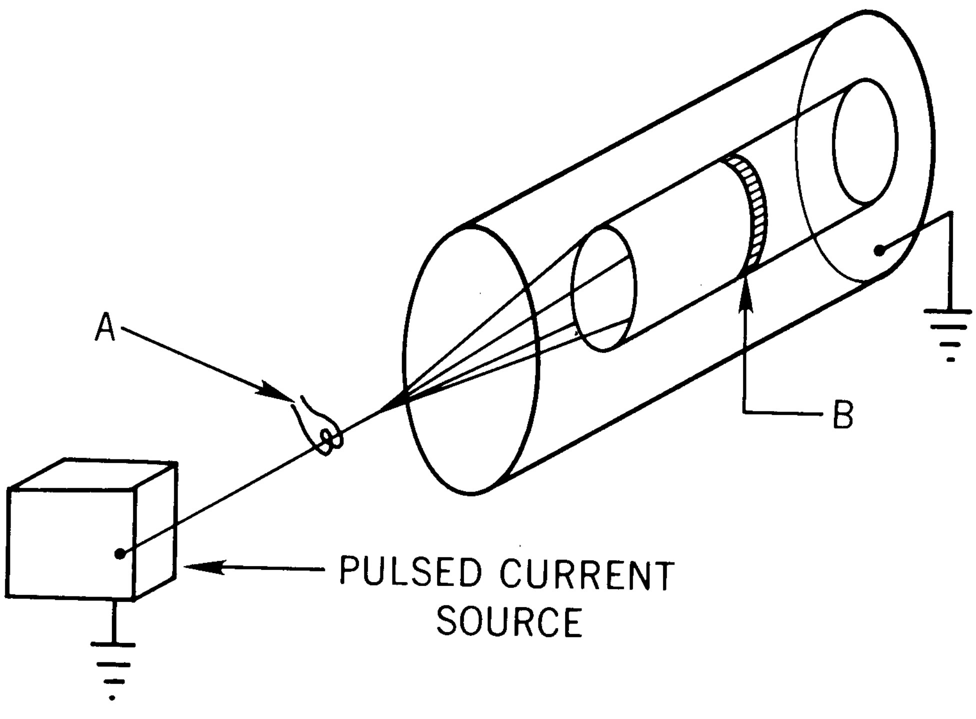

Figure 6. Bench test.

cylinder (location B). Comparison of measurements at locations A and B showed that the total axial current flowing on the inner cylinder was indeed the appropriate multiple of the current measured through one of the resistors.

The concentric-cylinder geometry was selected because it represented a symmetrical configuration within which the fields and currents could be readily calculated everywhere for a symmetrical excitation. Also, the outer cylinder served as an rf shield against external electromagnetic interference and as a containment vessel for the various media (dry air, N_2 vacuum, SF_6) under consideration. The data were compared with the calculated response of the inner cylinder obtained by using an assumed radiation distribution as input for the SAPSC computer code.

Several instruments were designed and deployed for this experiment: two one-turn Rogowski coils (to measure Compton current), a cathode follower, a special voltage probe (to make high-impedance voltage measurements), an emitter-follower circuit, and an E-field sensor (used by Denis Whittaker of HDL to measure the E-field).

The one-turn Rogowski coil (fig. 7) consists of a thin aluminum cylindrical outer container with a balanced output located at the center of the axis. The sensor is orientated so that the desired current component passes through the sensor parallel to the axis. The resulting magnetic (H-) field induces a current in the container and results in a voltage developed across the output; this voltage is proportional to the volume of the sensor and the time derivative of the Compton current. For this experiment, two sensors were constructed with volumes of 5×10^{-2} and 6×10^{-3} m^3.

The cathode follower, which had been used in the December test, was used again, except that considerably more radiation protection was provided in March. It was thought that this extra protection would minimize the transient-radiation effects on electronics (TREE) on the circuit components and that the device would operate as designed. The voltage to be measured was that generated on a Pb pig (a block of Pb), floating coaxially within a large outer cylinder (the same cylinder used for the coupling experiments).

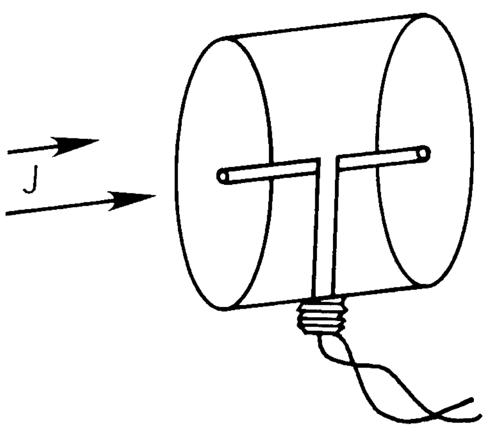

Figure 7. One-turn Rogowski coil ($\dot{J}$ sensor).

Tektronix voltage probes and specialized compensated voltage divider networks were used to drive the cathode follower, and the response was recorded on oscilloscopes in the data room.

Also, an emitter-follower circuit was used as an impedance matching driver in the same experimental configuration as that with the cathode follower. Further attempts to measure the voltage were made via a method suggested by Victor Van Lint (MRC) whereby a series of short-circuit and low-resistance current measurements was made, and the open-circuit voltage was inferred from the results.

Finally, during successive shots, an E-field sensor was placed at various locations near the floating pig, and the measured E-field was recorded. From these measurements, the total E-field, as a function of distance from the floating pig, could be determined and, from that, the voltage.

The third area of investigation concerns the basic phenomena and air chemistry associated with the source-region environment. For some time, certain air-chemistry parameters have been somewhat inadequately determined. Notable is the electron attachment rate in moist air. Data from a variety of investigations and compiled by Longley and Longmire* indicate that there is a major fluctuation in this parameter over the range of fields and pressures of interest for EMP. By these data, though, the measurements of electromagnetic environments resulting from nuclear tests do not agree well with the corresponding calculations (Conrad L. Longmire, MRC, private communication).

Consequently, it is desirable to obtain controlled experimental data from which the attachment rate can be reliably derived. To get these data, a "pie-pan" sensor was designed in collaboration with Longmire. The basic design (fig. 8) consists of a thin center plate which can be charged with an external power supply and capacitor network. The current discharged by the capacitor can be related to the phenomena which occur between the plates of the sensor when it is exposed to ionizing radiation. Attachment rates, recombination rates, conductivity, and the charge-depletion boundary layer can be studied in various gases by using this experimental setup. For this series of tests, two sensors were constructed, one with a plate separation of 2.54 cm and one with a plate separation of 5.08 cm.

Although all of the experiments conducted during this test series had some relation to tactical source-region simulation, the floating pig experiments provided direct insight into one of the field enhancement methods under active consideration. Gamma radiation and Compton currents build up the charge on conducting bodies which are thick to the incident ionizing radiation. This charge buildup results in an E-field which, perhaps, could be appropriately tailored to complement E-fields due to other mechanisms in a reasonable simulation of worst-case environments.

In the context of a long-term program, the March test was not meant to stand alone, but rather was designed to clear up some previous uncertainties and to begin investigation into some new areas. Examples are the current measurements on the truncated cylinder and the boundary-layer oriented pie-pan measurements. In general, the results of the March test contributed to a variety of areas.

**H. J. Longley and C. Longmire, Electron Mobility and Attachment Rate in Moist Air, Mission Research Corp. MRC-N-222 (12 December 1975).*

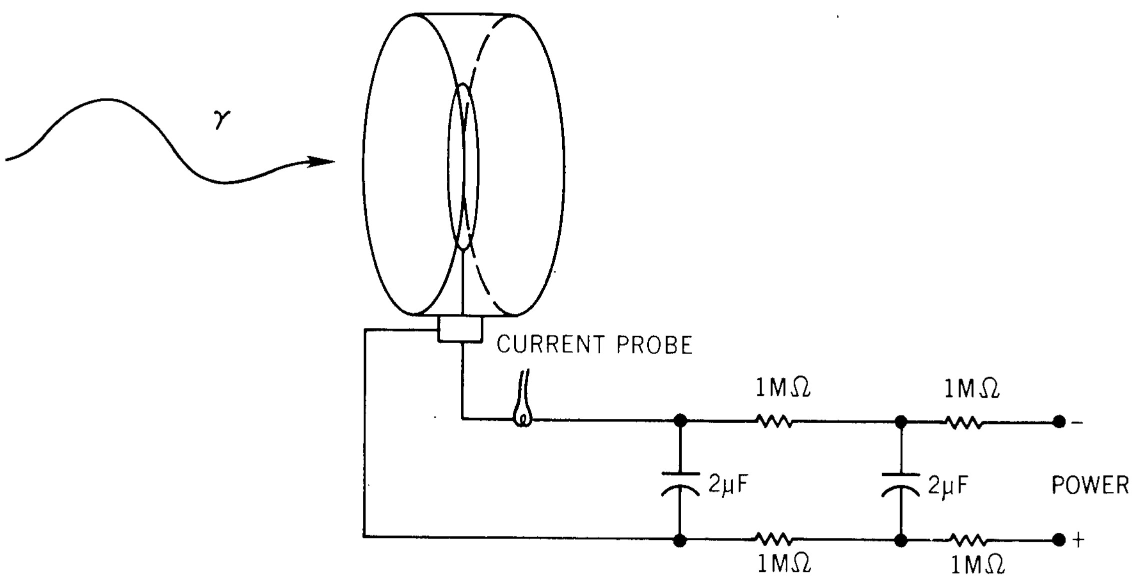

Figure 8. Pie-pan sensor.

2.3 Mission Research Corp./AURORA Memorandums

Conrad Longmire and William Crevier of MRC wrote four AURORA Memorandums in FY76: General Considerations on the Use of AURORA for Simulating EMP Coupling, Some Physics Experiments for AURORA, A Simple Analysis of the Blue Cylinder Experiment, and AURORA Boundary Layer Experiments. These AURORA Memorandums, along with Direct Interaction Effects in EMP,[2] form a collection of material that is a great help in understanding the possible uses of the AURORA Facility in source-region coupling experiments related to tactical situations of interest. Figure 9 shows an early example of a relatively simple AURORA modification, suggested by Longmire, that would convert the AURORA Facility into a partial simulator of the tactical source-region EMP. Longmire's modification would not provide an exact simulation of source-region EMP, but many of the important electromagnetic features of the source region would be partially simulated.

2.4 Code Development Contracts

Early in FY76, a contract was let to Science Applications, Inc. (SAI), to develop two computer codes and to provide the Government with a user's manual for these codes. Both of these codes solve Maxwell's

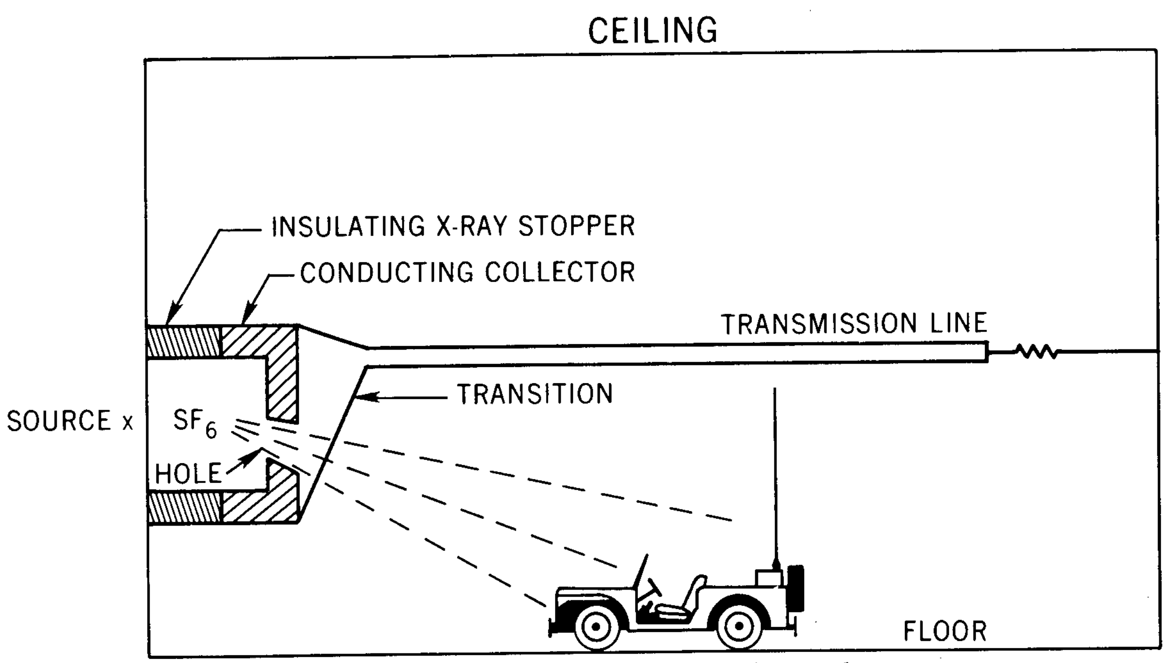

Figure 9. Possible simulation scheme.

[2]*C. L. Longmire, Direct Interaction Effect in EMP, Air Force Weapons Laboratory, EMP Interaction Note 69 (November 1973).*

equations in cylindrical coordinates, and both can analyze concentric cylinder geometries irradiated at the AURORA Facility. These codes provide the following types of output: electromagnetic fields, conductivities, and Compton currents in the region between the cylinders and the current coupled to the inner cylinder or the voltage generated between the outer cylinder and an electrically isolated inner body.

One of the codes uses a standard explicit finite-difference scheme to solve Maxwell's equations. It can treat the source electrons either self-consistently or non-self-consistently, allowing one to determine whether or not a self-consistent treatment is necessary for the analysis of AURORA experimental results. In addition, the self-consistent treatment will allow the code to operate for actual tactical source-region EMP environments if the effects of low-energy electrons can be neglected.

The other code uses an implicit finite difference scheme to solve Maxwell's equations. It can treat standard concentric cylinder geometries, and, in addition, configurations in which the cylinders are connected by lumped circuit elements (resistance, inductance, capacitance).

In addition to the computer codes, SAI will provide the results of four sample problems of HDL's choosing with the electron transport calculations used for each.

During FY76, work on the Maxwell equation equivalent circuit (MEEC) code progressed under contract with Intelcom Rad Tech (IRT), technically directed by Thomas Tumolillo of JAYCOR. The code is being developed for simulation studies and solves the Maxwell equations in rectangular Cartesian coordinates (by finite difference techniques) in a volume of air (or other gas) excited by Compton electrons in the presence of associated time-varying air conductivity.

The MEEC code is in the final phase of programming and debugging; that is, modification of the vacuum system generated EMP (SGEMP) version of the MEEC code to handle source-region effects of an ionized gas (typically air) is essentially complete. A flexible input language has been defined and coded in FORTRAN. The input language allows convenient access to all essential parameters entering the calculations. The coding associated with the calculation of air conductivity and the self-consistent tracking of source electrons (one available option) is complete. It is anticipated that the complexity of the entire modification of the MEEC code will require extensive and thorough testing and evaluation. In FY77, available AURORA experimental data will be compared with MEEC calculations.

2.5 Environment Code NEMP

The Army has sponsored the development of the NEMP computer code system, principally by Longley and Longmire, for prediction of EMP environments due to near-surface air bursts. After several years of effort, the code system (consisting of six codes run in sequence) is in a limited production status. The code system has been run to times of 5 ms by personnel of HDL using a rough EMP source package for a 200-m height of burst. Some further work will be done by MRC in FY77 to verify the correctness of the computed fields and to examine fields extrapolated outside the source region.

The Army has sponsored also Monte Carlo transport studies by M. O. Cohen of the Mathematical Applications Group, Inc. (MAGI), to obtain predictions of EMP sources due to neutron-induced secondary gamma rays for burst heights of 50 and 100 m. These predictions are of a higher quality than heretofore available, especially near the air-ground interface. Additional studies by MAGI of more general neutron spectra are planned for FY77.

Meanwhile, HDL is developing a NEMP output graphics code and is performing analytic curve fitting of the MAGI transport results for inclusion in the NEMP code system. Also, HDL has brought the NEMP system to a production status on the HDL computer, an IBM 370/168 system, in addition to the Control Data Corp. (CDC) 7600 system on which the NEMP code was developed.

2.6 Interaction and Coupling Analyses of Lance Missile System and AN/GRC-106 Radio System

The EMP survivability criteria for tactical endoatmospheric nuclear threats differ significantly from those for exoatmospheric threats because of several factors:

a. The presence of ionizing radiation, Compton current density, and time-varying conductivity for endoatmospheric threats

b. The "near-zone" character of the electromagnetic field for endoatmospheric threats as opposed to the radiated plane wave character for exoatmospheric threats

c. Relatively large field strengths of certain components at times beyond 1 μs or so for endoatmospheric threats.

Furthermore, from preliminary analyses of isolated interaction and coupling mechanisms, it can be argued that these differences between EMP survivability criteria for exoatmospheric and tactical endoatmospheric nuclear threats can lead to significantly different interaction and coupling phenomena.

Going one step further, some voids can be identified in the existing technology base--that is, technology developed specifically for tactical endoatmospheric threats, technology developed for strategic endoatmospheric threats and applicable also to tactical situations, and technology developed for exoatmospheric threats and easily modified to account for certain "weak" source-region effects. These voids can be identified through vulnerability assessments of actual tactical systems; these assessments are attempted in sufficient detail to illuminate such technology voids. The interaction and coupling analyses of the Lance Missile System and the AN/GRC-106 Radio System were performed, therefore, according to the following approach:

a. Define principal response mechanisms and critical circuits for both systems with respect to the tactical source-region environmental factors listed in the first paragraph of this section.

b. Develop worst-case idealized representations of principal response mechanisms, and define the state-of-the-art theoretical methods which can be applied with the most confidence in the system analyses.

c. Predict responses of principal interaction and coupling mechanisms and the corresponding source impedances which are necessary to assess susceptibilities of critical circuits to damage.

d. Develop techniques and design tests which will provide experimental verification of these theoretical predictions; consider underground nuclear tests, flash x-ray machines, electron-beam machines, and current injectors.

e. Identify voids in existing theoretical and experimental technology which seriously impede meaningful susceptibility and vulnerability assessments.

The interaction and coupling analyses of the Lance Missile System and the AN/GRC-106 Radio System were conducted under an Army-sponsored contract.[3,4] Four types of excitation of each system were considered:

a. Electromagnetic excitation (electromagnetic field and transient air conductivity) of external cables and antennas

b. photon excitation of external cables

---

[3] *R. A. Perala et al, Coupling Calculations for the LANCE Missile System in a Tactical Nuclear Environment (U), Mission Research Corp. Report No. AMRC-IR-76457 (March 1976). (SECRET RESTRICTED DATA).*

[4] *R. A. Perala et al, Close-in Coupling Analysis of the AN/GRC-106 Radio System (U), Mission Research Corp. Report No. AMRC-IR-76458 (March 1976). (SECRET)*

c. Electromagnetic excitation of internal cables due to internal EMP (IEMP)

d. Electromagnetic excitation of internal cables due to apertures in enclosures

The contractor's results from the interaction and coupling analyses of the Lance Missile System and the AN/GRC-106 Radio System have been used at HDL to assess the susceptibility of critical circuits to damage.[5]

3. TECHNICAL MILESTONES

Throughout FY76, technical efforts were directed toward specific goals outlined in section 1. Significant progress has been made and, as a result, some definitive statements can be made in several technical areas. These areas include boundary-layer phenomena, Compton current measurements, E-field measurements, voltage measurements, and gamma-thick charging phenomena.

This section does not completely describe all of the technical work undertaken during FY76, but discusses only those topics about which some conclusions or significant results have been obtained.

3.1 Boundary-Layer Conclusions and Results

Longmire[2] and Baum[6] considered the development of an electron depletion layer between a negatively charged conductor and a collision dominated plasma. As shown in figure 10, when a metallic electric conductor is negatively charged, the resulting E-field is in a direction to remove electrons from the metal surface; however, no electrons are removed from the metal surface. Electrons cannot be emitted because the E-field ("E" in fig. 10) is not large enough to produce high-field emission, a phenomenon that occurs only at extremely high E-field intensities. To be specific, experimentally it has been found and theoretically it may be shown that the high-field emission current density, J_{hf}, is given by

$$J_{hf} = CE^2 \exp(-K/E) \quad ,$$

---

[2] *C. L. Longmire, Direct Interaction Effect in EMP, Air Force Weapons Laboratory, EMP Interaction Note 69 (November 1973).*

[5] *Daniel L. Goodwin, The LANCE Electromagnetic Pulse (EMP) Assessment--Endoatmospheric Threat (U), Harry Diamond Laboratories TM-77-14 (October 1977). (CONFIDENTIAL)*

[6] *C. E. Baum, Radiation and Conductivity Constraints on the Design of a Dipole Electric Field Sensor, Air Force Weapons Laboratory EMP Sensor and Simulation Note 15 (June 1970).*

where, for a tungsten emitter, the constants C and K are given by

$$C = 1.26 \times 10^5 \text{ A/V}^2 ,$$

$$K = 2.76 \times 10^{10} \text{ V/m} .$$

At 10^6 V/m,

$$J_{hf} = 1.26 \times 10^5 \times 10^{12} \exp\left(-2.76 \times 10^4\right) \tag{1}$$

$$\approx 0 .$$

The foregoing equation holds only for perfectly clean flat surfaces. Microscopic irregularities can cause extremely high local E-fields which can sometimes cause enough current to produce local hot spots. Thermionic emission can then occur. One of the reasons for conducting the pie-pan experiments is to see if electron emission does or does not occur by some such mechanism. If electron emission does not occur, a region of positive ions results. As indicated in figure 10, a rather intense E-field connects these positive ions with the electrons in the metal.

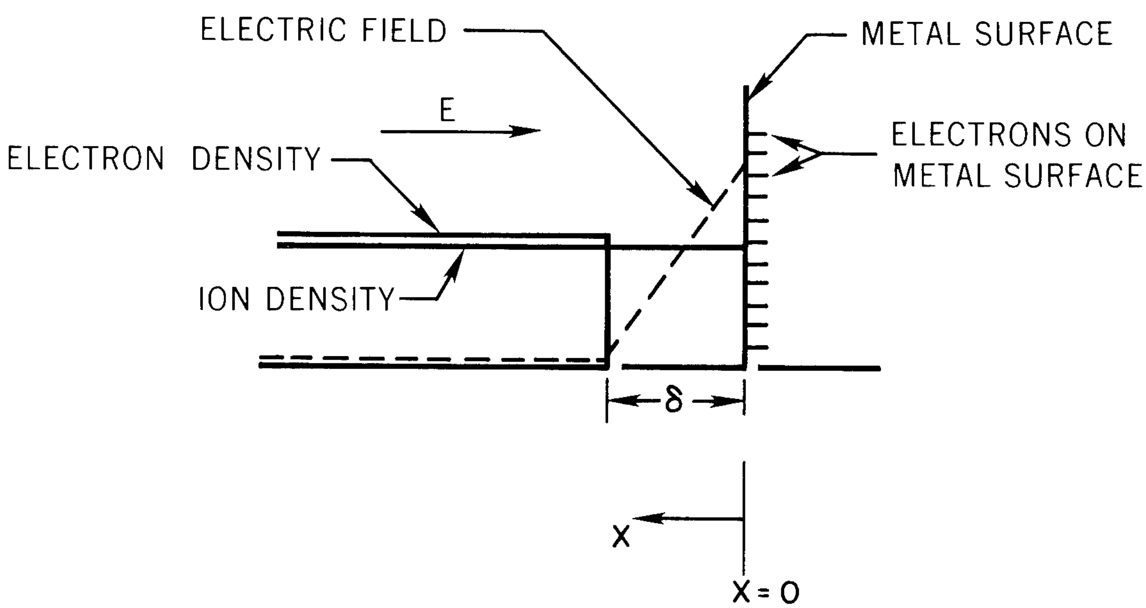

Figure 10. Model of boundary layer.

Consider the situation when the sensor shown in figure 11 is filled with N_2 gas and subjected to an AURORA radiation pulse. If one neglects the boundary layer and applies conventional wisdom, current should flow through the chamber as long as the N_2 gas remains ionized. By using accepted electron-positive N_2 ion recombination rates, the N_2 gas should remain ionized much longer (milliseconds) than the duration of the AURORA pulse (300 ns).

When the chamber was subjected to the AURORA ionizing radiation pulse, current flowed through the chamber only for a time approximately equal to the duration of the AURORA pulse. The short duration of the current pulse is consistent with the formation of an electron depletion region or boundary layer at the center of the negatively charged electrode. If there were no boundary layer formed at the inner conductor, current would flow for times up to milliseconds, that is, until all the electrons recombined with the positive nitrogen ions.

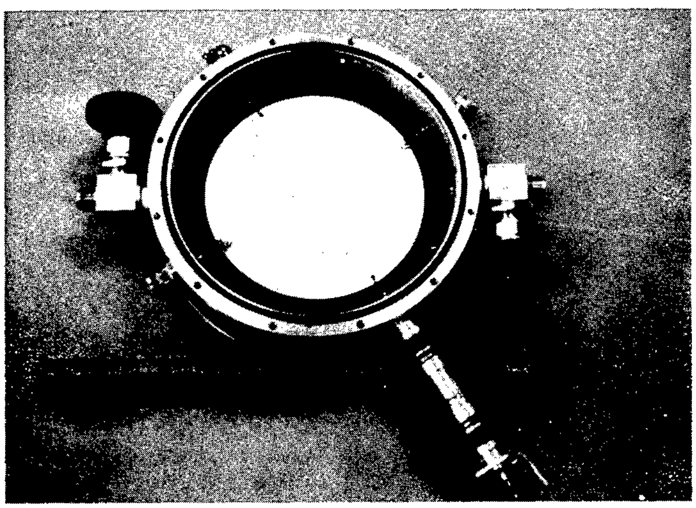

Figure 11. Pie-pan sensor.

Crevier and Longmire (MRC, unpublished data) have developed a quantitative theory to explain the behavior of the sensor when subjected to the AURORA pulse. Essentially, the current that flows through the sensor is set equal to

$$\dot{q} = i(t) = \sigma(t)E(t)A \ , \tag{2}$$

where i(t) is the current, $\sigma(t)$ is the ionized gas conductivity, E(t) is the E-field outside of the plasma boundary layer, and A is the area of the plate. Then

$$\dot{q} = \frac{V_p - V_{b\ell}}{D} \quad \mu e N_e A = \sigma E A \ , \tag{3}$$

where V_p is the voltage across the sensor plates, $V_{b\ell}$ is the boundary-layer voltage across the electron depletion layer, D is the distance between the plates, μ is the electron mobility, e is the electric charge of an electron, and N_e is the electron number density.

Voltage $V_{b\ell}$ is given by the integral of the E-field $E_{b\ell}(x)$ across the electron boundary layer:

$$E_{b\ell} = -\frac{V_p}{D} - 4\pi e N_+(\delta - x) \ , \tag{4}$$

where is assumed to be a relatively sharp cutoff of the boundary layer. Then

$$V_b = \int_{\delta}^{0} E_{b\ell}(x)\ dx \ . \tag{5}$$

The charge, q, per unit area on the negatively charged conductor can be set equal to the charge in the boundary layer. Then

$$q = eN_+\delta A \ , \tag{6}$$

or

$$\delta = \frac{q}{eN_+} \ ,$$

and

$$E_{b\ell} = -\frac{V_p}{D} + 4\pi(eN_+\delta)\left(\frac{x}{\delta} - 1\right) \ ,$$

or

$$E_{b\ell} = -\frac{V_p}{D} = 4\pi q\left(\frac{x}{\delta} - 1\right) \ . \tag{7}$$

Then follows

$$V_{b\ell} = \int_{\delta}^{0} E_{b\ell}\, dx$$

$$= - V_p \frac{\delta}{D} + 4\pi q\left(\frac{x^2}{2\delta} - x\right) \Bigg|_{x=\delta}^{x=0}$$

$$= + V_p \frac{\delta}{D} + 2\pi q\delta$$

$$= + V_p \frac{\delta}{D} + \frac{2\pi q^2}{eN_+} \ . \qquad (8)$$

The fraction δ/D is much less than 1, so

$$V_{b\ell} \equiv \frac{2\pi q^2}{eN_+} \ .$$

Equation (3) then becomes

$$\dot{q} = \frac{\mu e N_e}{D}\left(V_p - \frac{2\pi}{eN_+} q^2\right) A \ , \qquad (9)$$

where the electron mobility is given by

$$\mu = 7.33 \times 10^5 \ E^{-\frac{1}{2}}$$

for $0.1 < E < 10$ electrostatic units. One can insert the proper N_2 gas chemistry to obtain the results shown in figure 12.

The pie-pan sensor has been used to study the conductivity and boundary-layer effects in a number of pure gases and mixtures of gases for E-fields up to 80,000 V/m. The gases studied have been dry air, N_2, O_2, SF_6, and, finally, "humid" air with humidities ranging from 0 to 100 percent at 36°C.

When a specific gas was studied at a specific dose level, current pulse measurements corresponded to 2000, 1000, 300, 100, and 10 V applied to the sensor.

The experimental technique used in obtaining the 100-percent saturated humid air (at temperature T) was to bubble dry air through two flasks in series containing water at temperature T. The pipes, hoses,

N_2 , AIR (DRY AND WET)

O_2 , SF_6

$I = AN_eV_e \approx$ TENS OF AMPERES

IN AIR $\quad N_e = \dot{\gamma}/\alpha_e$

$$V_e = \mu_e E$$

$$I \propto \dot{\gamma}\mu_e/\alpha_e$$

$$E = \frac{V_p - V_{b\ell}}{D}$$

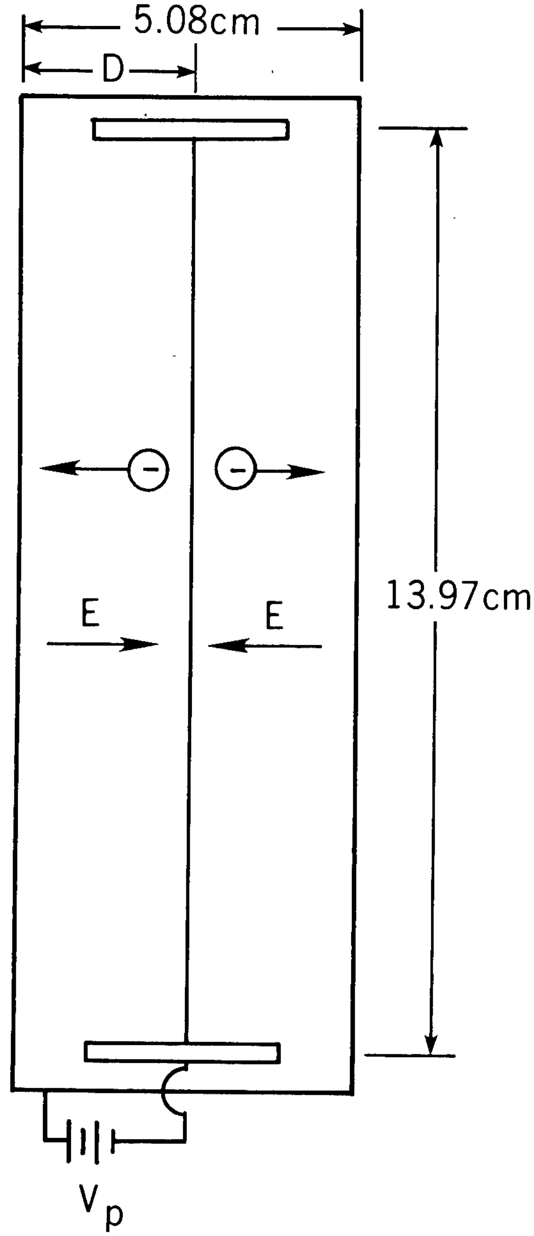

Figure 12. Pie-pan model (used in W. Crevier and C. Longmire calculation, Mission Research Corp.).

and pie pan were kept at a temperature about 5° to 10°C hotter than the water. The setup is depicted in figure 13. Since the sensor was at a temperature greater than T, water did not precipitate in the sensor. Figure 14 shows a schematic drawing of the experimental setup during an AURORA shot.

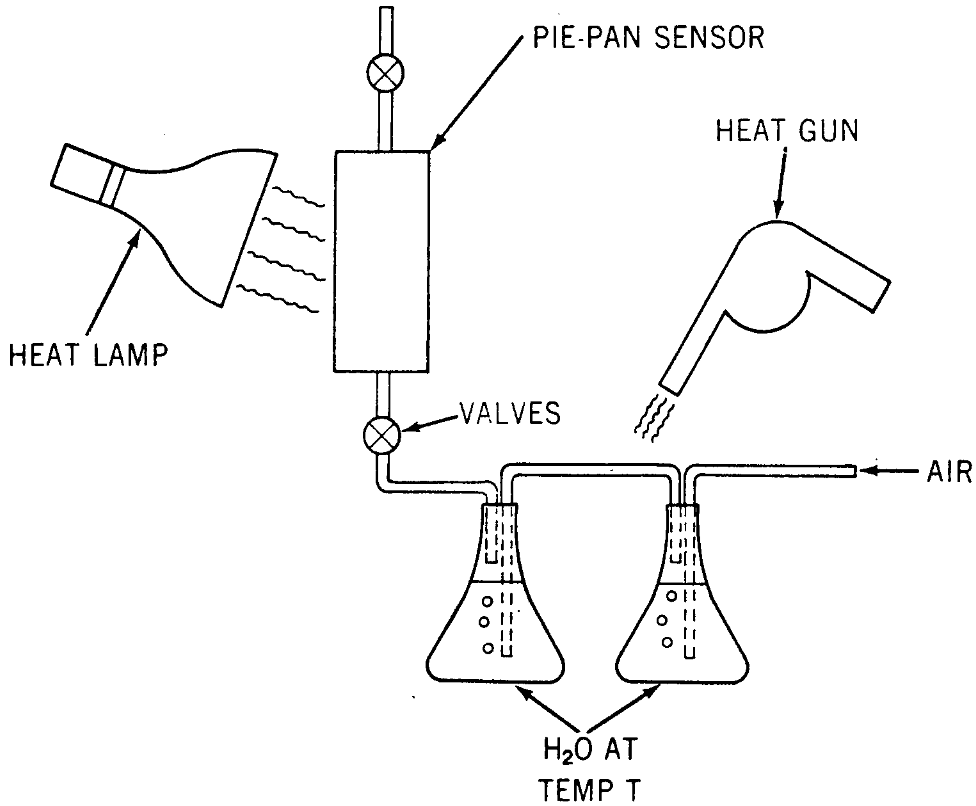

Figure 13. Method of filling pie-pan sensor with humid air.

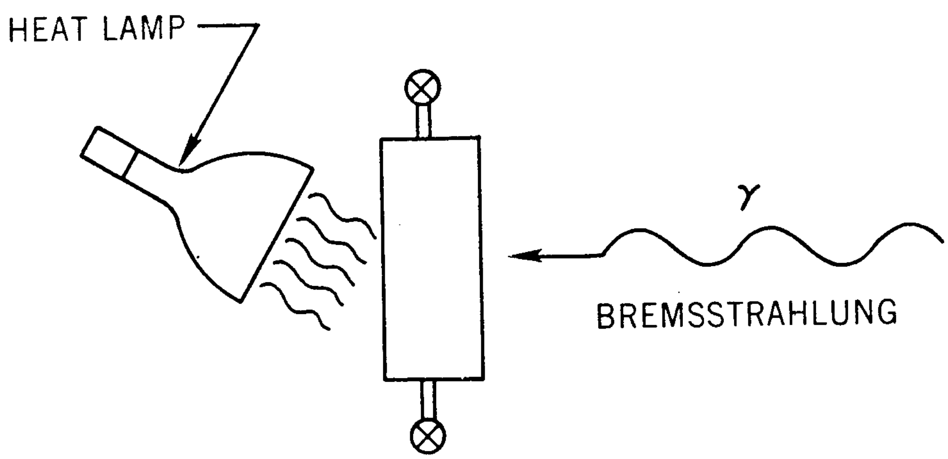

Figure 14. Method of preventing H_2O precipitation if humid air is 100-percent saturated at temperature T and sensor is heated to temperature T_s, where $T_s \geq T + 5°C$.

The dry-air and N_2 experimental data have been reduced, and sample comparisons between the theoretical responses and the measured data are given in figure 15. The O_2, SF_6, and humid-air data have not yet been corrected for cable losses, etc. However, the conductivity of the 100-percent humid air at 50°C is about 4.5 times less than that of dry air.

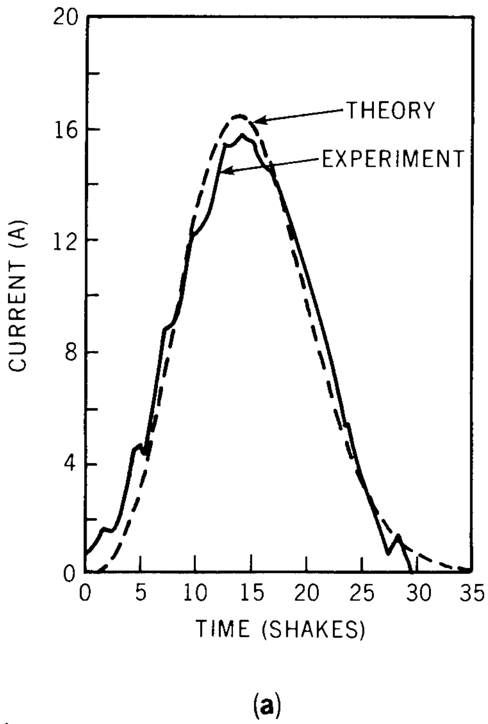

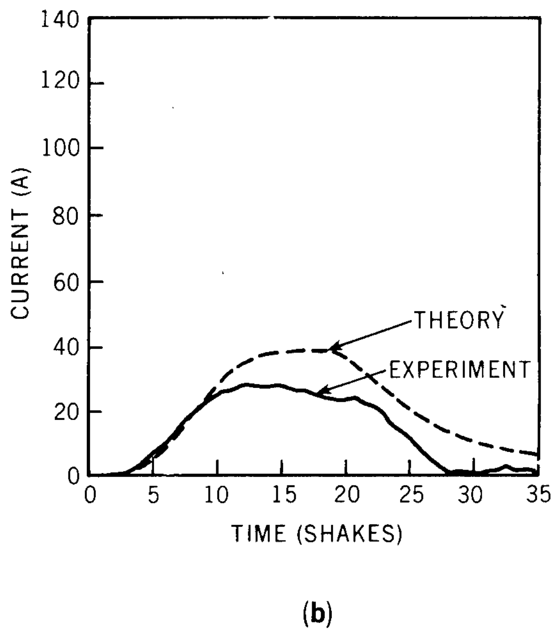

Figure 15. Pie-pan response: (a) dry air and (b) nitrogen (bias: 1000 V).

3.2 Compton Current Measurement

One of the stated goals of the FY76 experimental effort was to measure the "free" electromagnetic environment in the AURORA test cell during the radiation pulse. One important parameter to be considered was the Compton current. Several different instruments were considered, and data were obtained by using each. These included the Compton diode (which has been used extensively for underground tests), the Rogowski coil type of current probe (both in a special collimated configuration and as an off-the-shelf item), and the one-turn Rogowski coil. Measurements were made during the December and March AURORA tests, and the significant results were compiled for all of the data.

The Compton diode, although it has been demonstrated to be a powerful experimental tool, has two inherent problems. One is that, to be sensitive to small current densities, it must be large. Another is that it collects current indiscriminately and must be collimated and shielded if one is to determine the vector current density at any location. These two problems act in opposition. Experience during FY76 indicated that these problems would be extremely difficult to solve. The Compton diode with which data were taken was designed so that a reasonable signal should be obtained while size and shielding were kept to a minimum. The reason for this size restriction was that once a reliable means of measuring Compton current was determined, the AURORA test cell would be mapped. The sensor, therefore, had to be small and portable to map the test cell. The initial data obtained by using the sensor showed signals which were buried in the noise. Attempts to increase the sensitivity of the sensor by changing the resistance divider in the output failed to produce reasonable results. The total dose on the front of the sensor (measured by using TLD's) indicated that adequate Compton current should be reaching the sensor, but the cable noise level was such that meaningful results could not be obtained. Consequently, either (1) considerable effort would have to be undertaken to increase the sensitivity or reduce the noise or (2) the general approach could be abandoned for the time being in favor of pursuing other concepts. The latter pursuit was chosen.

The Compton current was measured also by using ADELCO current probes of 4.3-cm diameter. Reasonable measurements of the Compton current could be made inside the concentric cylinder geometry (where the probe was afforded considerable rf shielding), but in the AURORA test cell itself, results were inconsistent. As with the Compton diode, collimation is required to measure one vector component of the current density at a location. When the collimator was used during the December test, the signal was reduced to the level that noise problems were overwhelming. When the collimator was removed during the December test, however, the measurements were within 20 percent of the predicted values. Unfortunately, the measured values were neither consistently greater nor less than the predicted values, and during the March test there was little correlation between the theoretical and the experimental values. This lack of correlation may be due to the fact that the ADELCO probes measure the total current (not just the Compton current) passing through them, and the Compton current could not be separated from the conduction current. Enclosing the current probe with an aluminum can filled with SF_6 would prevent conduction current from passing through the current probe and might allow a successful Compton current measurement with this type of probe. Also, varying the thickness of the can could provide information concerning the energy spectrum of the electrons produced in the AURORA test cell. During the March test, a larger ADELCO probe (13.3-cm diameter) was used, but measurements were not successful more than 2 m from the hot spot.

Longmire suggested (unpublished) the one-turn Rogowski coil as a means of measuring the Compton current. Further refinements in the original design resulted in a sensor that measured the Compton current with no requirement for collimation. In addition, the differential output minimized the noise problems. Two models of the sensor were constructed and used during the March test. Data were taken by using the small sensor over a range of dose rates from 10^9 to 10^{11} rads (Si)/s, but the sensor response was not as predicted. Careful consideration of the data indicated that the sensor was not sensitive enough, considering the noise levels, for AURORA application. The larger sensor provided reasonable results over that dose rate range. Peak amplitudes of the integrated reduced data compared favorably with the predicted peak Compton current density of $J = -2 \times 10^{-8}\ \dot{R}\ A/m^2$, where $\dot{R}$ is the dose rate in rads (Si)/second (fig. 16). Comparison of the integrated pulse shape with the AURORA radiation pulse (appropriately scaled) (fig. 17) is similarly good. The discrepancies between the measured and predicted data seem to be most prominant in the lower radiation region indicating that 10^9 rads (Si)/s is probably the lower limit of the response range of the sensor. Since the response of the sensor is proportional to its volume, use of a larger sensor should extend the range over which measurements can be valid.

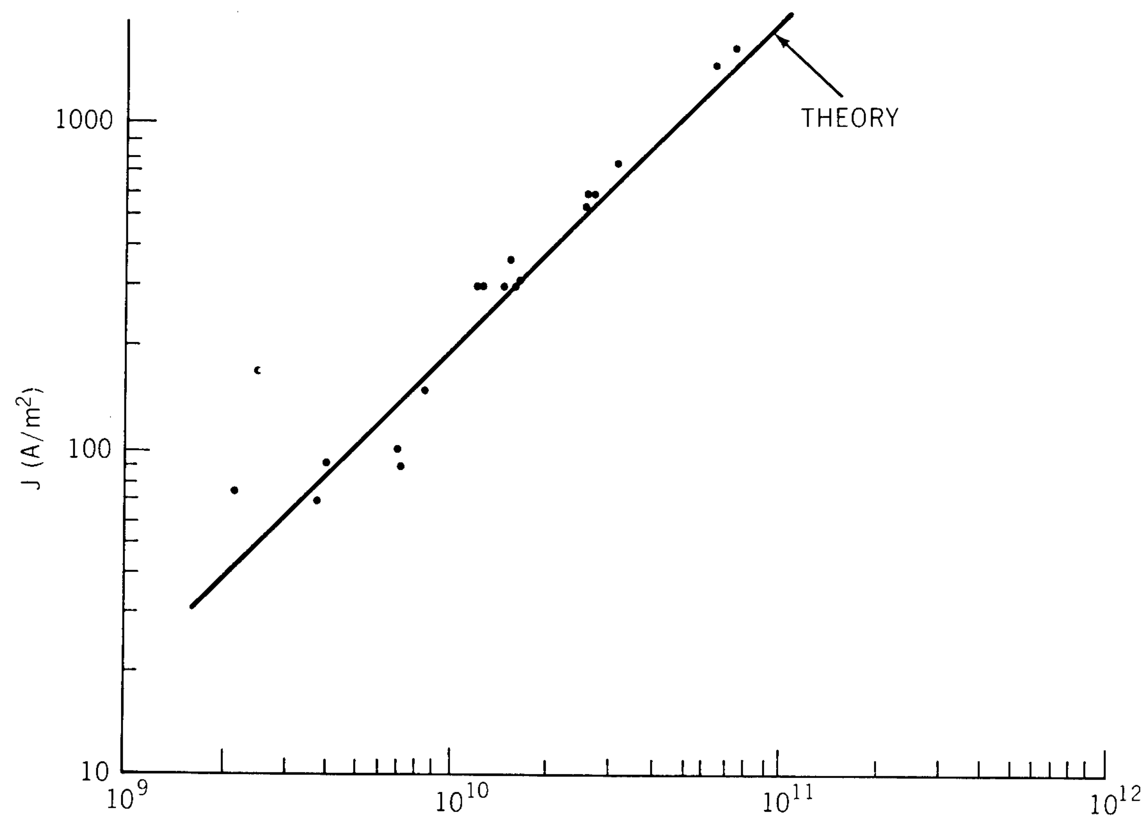

Figure 16. $\dot{J}$ sensor.

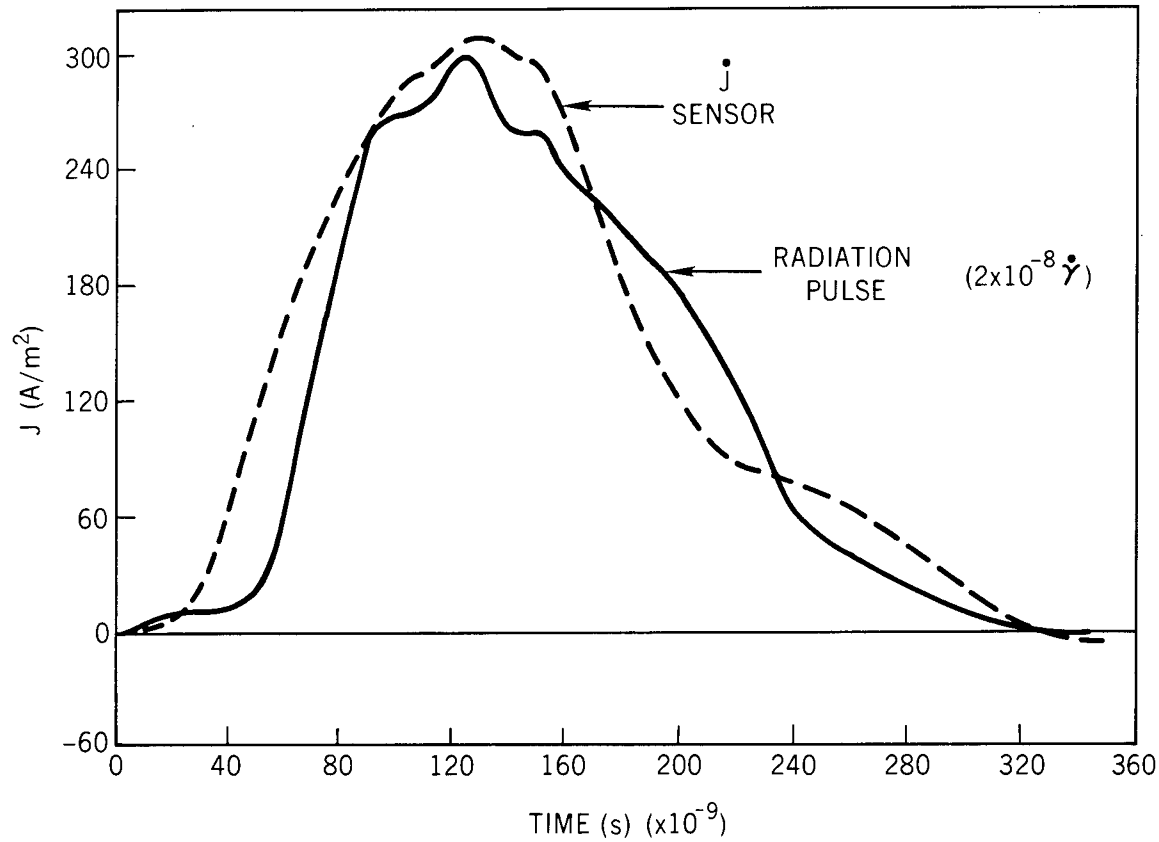

Figure 17. Compton-current time history.

In conclusion, use of the one-turn Rogowski coil sensor seems the most adequate method of measuring the Compton current in the AURORA test cell. In the future, a larger, more sensitive model will be constructed. By its use, the Compton current spacial distribution within the AURORA test cell can be fully characterized.

3.3 Electric-Field Sensor

The measurement of the E-field in a medium that has a time-varying conductivity, such as the ionized air present in the AURORA test cell, has proved to be difficult. Consider a parallel plate sensor (with plates separated a distance d) that is placed with the plates perpendicular to the E-field (fig. 18). Let the load across the plates be resistance R. Conservation of current then yields

$$A\sigma E - A\varepsilon \frac{dE}{dt} = A\sigma E' + A\varepsilon_o \frac{dE'}{dt} + \frac{AE'd}{R} , \tag{12}$$

or in terms of the voltage, V, across R, assuming that the value of E is not changed by the presence of the sensor,

$$A\sigma E - A\varepsilon_o \frac{dE}{dt} = \frac{A\sigma V}{d} + \frac{A\varepsilon_o}{d}\frac{dV}{dt} + \frac{VA}{R} \tag{13}$$

or

$$-\frac{dE}{dt} + \frac{\sigma(t)}{\varepsilon_o} E = \frac{\sigma(t)}{\varepsilon_o d} V + \frac{1}{d}\frac{dV}{dt} + \frac{V}{A\varepsilon_o R} \; . \tag{14}$$

The solution of this differential equation is given by

$$E = \exp\left[\int_o^t \frac{\sigma(t')}{\varepsilon_o}\, dt'\right] \cdot \int_o^t (A \cdot B)\, dt' \;, \tag{15}$$

where

$$A = \exp\left[\int_o^{t'} \frac{\sigma(t'')}{\varepsilon_o}\, dt''\right] \;,$$

$$B = \frac{1}{d}\frac{dV}{dt'} + \frac{\sigma(t')}{\varepsilon_o}\frac{V}{d} + \frac{1}{A\varepsilon_o R} V(t') \quad .$$

This is a rather unwieldy expression and, unfortunately, it is difficult to simplify under AURORA conditions. Specifically, the AURORA has a rise time of 10^{-7} s, but $\varepsilon_o/\sigma = 10^{-11}/10^{-4} = 10^{-7}$ s, and so both dV/dt and V significantly contribute to the determination of E.

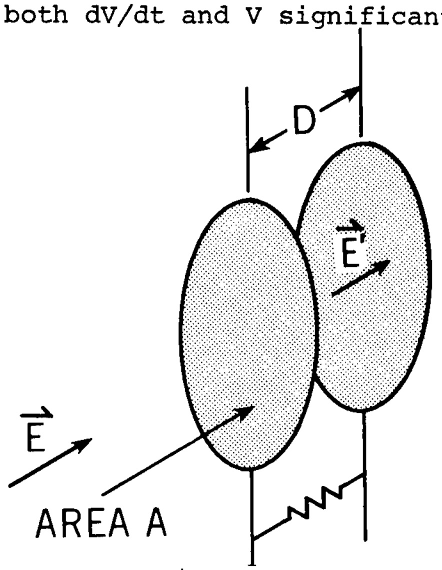

Figure 18. Electric-field sensor.

Furthermore, if a boundary layer or electron depletion layer forms between the ionized air and the negative plate of the sensor, equations (12) and (15) can be oversimplifications. If R can be made large enough by use of a high input impedance cathode or emitter follower, the plates of the E-field sensor could not collect charge, and the boundary layer phenomena would be kept to a minimum.

Up to the present, a great deal of the work done on E-field measurement in the presence of ionizing radiation has been devoted to situations involving soft x rays. Workers have gone to great efforts to reduce the photoelectric interaction between the E-sensor plates and the ambient ionizing radiation. To reduce the possibility of electron emission by the photoelectric effect or by the Compton effect, screens have been substituted for solid plates. To even further reduce the photoelectric electron emission, the screens have been constructed of light, low-atomic-number materials.

The substitution of screens for plates does certainly reduce direct electron knockout by low-energy bremsstrahlung or x rays, but the small area of the screen plates creates another severe problem by enhancing the boundary layer. The boundary layer is enhanced by screens or grids because large E-fields can build up around the small wire or sharp corners of the grid plate.

To be more specific, it can be argued that the voltage across the boundary layer varies as

$$V_b = 1/(\text{surface area})^2, \tag{16}$$

where the surface area refers to the actual electrically dense area of the grid. Grids, therefore, may increase the boundary layer problem. Thin aluminum or copper solid foils may, therefore, have an advantage over grids in constructing the E-field sensor for the AURORA environment. Fortunately, the AURORA bremsstrahlung spectrum is relatively hard, and emission of photoelectrons from the parallel plates may not be important.

3.4 High-Impedance Voltage Measurements

It was recognized early in the program that a successful method of making a high-impedance voltage measurement in the AURORA radiation environment would have wide application to include E-field measurements, coupling measurements, and system response measurements. Initial investigation showed that simple resistance divider networks were plagued by two problems: the requirement for capacitive compensation and loss of signal amplitude. These problems exist in proportion to the impedance over which one attempts to measure; the higher the impedance, the greater the signal loss and requirement for compensation. It was indicated that these problems could be greatly reduced by using a cathode follower circuit network, which has a gain of somewhat near unity, but can match high-impedance loads to low-impedance cables. Cathode-follower circuits, rather than emitter-follower circuits, were initially chosen because tubes are generally thought to be less troubled by ionizing radiation than are solid-state components.[7]

During the experiments at AURORA during FY76, high-impedance voltage measurements were made by using cathode followers: one method

[7] P. A. Trimmer, *Transient Radiation Effects on Basic Triode Amplifiers*, Harry Diamond Laboratories TR-1197 (April 1964).

used a Tektronix voltage probe, and a second method used a breadboard compensated voltage divider network.

3.4.1 Method 1

A cathode-follower circuit (1-MΩ input impedance) served as an interface between a Tektronix P6003 voltage probe and a 75-Ω data cable. A radiation-induced voltage source was sensed by the probe and was recorded from oscilloscopes.

After review of the data, which included several noise measurements, it was concluded that two problem sources prevented successful voltage measurement by method 1: radiation-induced ionization near the tube and radiation interaction with the voltage probe. The ionization near the tube could be minimized by adding more radiation shielding to the circuit. The interaction with the probe could be minimized in the same manner, but more shielding would add considerable stray capacitance, carry the high-voltage signal a great distance, and render the probe inconvenient.

3.4.2 Method 2

Method 2 was similar to method 1, except that the Tektronix voltage probe was replaced with a breadboard compensated voltage probe constructed for this application. As with method 1, the voltage was sensed by the probe and recorded from oscilloscopes.

The failure of method 2 to provide meaningful data was attributed to improper compensation of the voltage probe, due probably to unaccounted-for stray capacitance in the experimental configuration.

Victor van Lint (MRC) indicated that an emitter follower could be designed which could work in the radiation environment. Subsequently, an emitter follower, built to his specification, was constructed, but the results obtained by using it seem inconclusive.

Also, van Lint suggested another measurement method by which the open-circuit voltage can be determined without actually being measured directly. The method requires two current measurements, first with the monitor point short-circuited to ground and then with the monitor point connected to ground through a variety of small resistors. When the peak currents measured are plotted as a function of resistance, the open-circuit voltage can be inferred. This method was tried, but the result was somewhat different from that predicted by Van Lint. The voltage of the gamma-thick body in the experiments may have been influenced by boundary-layer effects so that a determination of the open-circuit voltage would require additional analysis.

Measurements of high-impedance voltage in the AURORA radiation environment remain inconclusive.

3.5 Interaction and Coupling Theory

3.5.1 Rectangular Configuration

In the December test, a simple quasi-static model was used to predict (1) the voltage generated between the inner and the outer boxes when they were electrically isolated and (2) the current flowing between the inner and the outer boxes when they were connected by a wire.

For the voltage calculations, the configuration was treated as a capacitor being charged. The total charge flowing between the boxes due to any conductivity in the region between the boxes was subtracted from the total charge deposited on the inner box due to the Compton current. The resultant charge, Q, was used in the equation $V = Q/C$ to obtain the voltage generated between the boxes. Since the voltage measurements were unsuccessful, no comparisons between these calculations and actual measurements were possible.

For the current calculations, the current flowing between the boxes was assumed to be due entirely to the Compton current intercepted by the inner box, and electromagnetic effects were neglected. As seen in table I, the results of these calculations reasonably agree with experimental results despite the fact that only direct interaction effects were considered. These calculations are reasonably accurate only because the wire connecting the inner and the outer boxes was perpendicular to the direction of the Compton current flow. If this wire had been in the same direction as the Compton current, the H-field created by the Compton current would have had a significant effect on the coupled current measured. Thus, simple quasi-static models which consider only direct interaction effects may be quite useful in understanding certain interaction and coupling phenomena observed in AURORA experiments.

TABLE I. PEAK COUPLED CURRENT

$\dot{\gamma}$ (10^9 rads (Si)/s)	Type	Experimental current (A)	Theoretical current (A)
3.92	Thick	1.26	1.82
3.53	Thick	1.28	1.63
2.92	Thin	0.28	0.32

3.5.2 Concentric Cylinders

In the March test, the computer code SAPSC was used to predict the current coupled to the truncated inner cylinder. This code uses a finite-difference scheme to solve Maxwell's field equation in a radiation environment. The Compton source distribution used in the calculations has a spacial and an angular distribution given by $(\cos\theta)/R^2$, where θ is the angle between the path of a Compton electron and the axis of the concentric cylinders, and R is the distance to the center of the AURORA hot spot. The measured data and the output of this code can be compared in figure 19. Theory and experiment disagree somewhat. Two possible improvements in the theoretical treatment are (1) the use of more accurate Compton source distributions and (2) the incorporation of boundary-layer phenomena. The POEM output, which SAI is under contract to deliver to HDL, should provide the former improvement, and work is presently being done on the latter one.

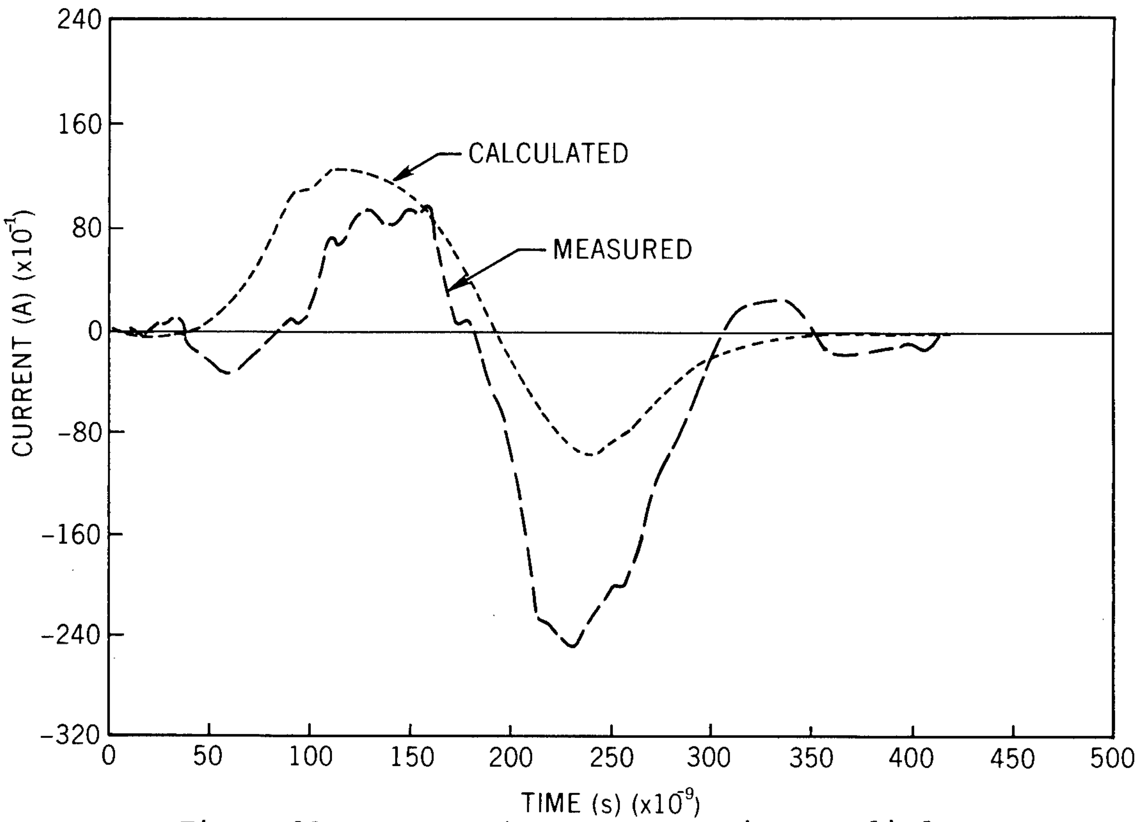

Figure 19. Total axial current on inner cylinder.

3.6 Direct versus Electromagnetic Coupling Mode Dominance

The agreement between the crude quasi-static calculation of the current and the measured current in the concentric box experiment may appear trivial. But a calculation that is based on a simple equivalent circuit, neglects inductive couplings, and yields a reasonable answer is useful in the estimation of tactical source region coupling. A purely capacitive quasi-static approach to the estimation of the measured current is valid probably because the wire between the absorber and the wall of the outer cubic chamber is essentially perpendicular to both the Compton current and the H-field resulting from the Compton current.

The amount of magnetic energy in the outer box is appreciable, but the inductive coupling between the inner gamma-thick absorber and the H-field is very small. The magnetic energy in the outer container can be estimated. The inductance per unit length due to the partial flux linkages within a round wire can be shown to be

$$L = \mu_o/8\pi \ , \tag{17}$$

where μ_o is the permeability of free space. If the square outer box is approximated with a round box of equal area, the inductance of the Compton current passing through the box is given by

$$L = \left(\mu_o/8\pi\right)\ell \ , \tag{18}$$

where ℓ is the length of the box parallel to the Compton current. One can compare the magnitude of the capacitive energy between concentric boxes and the magnetic energy in the outer box. That is, $\frac{1}{2}CV^2$ can be compared with $\frac{1}{2}LI^2$. The Compton current through the box is $I = JA_o$, where J is the Compton current density, and A_o is the area of the outer box.

The energy found is

$$\tfrac{1}{2}CV^2 = 2.05 \times 10^{7} \text{ joules} \ , \tag{19}$$

and

$$\tfrac{1}{2}LI^2 = 2.50 \times 10^{-6} \text{ joules} \ . \tag{20}$$

In other words, a significant amount of energy is stored in the H-field, but the energy is not being coupled into the wire between the concentric cubes.

In the March tests, the geometry consisted of a cylindrical gamma-thick absorber inside an outer cylinder. The absorber was connected by wire to the end plate (fig. 20). The resulting current measurements were about 5 to 10 times larger than those calculated with simple quasi-static models that neglect inductance. In this geometry, however, the wire connecting the absorber to the outside container was parallel to the Compton current. Magnetic flux lines encircled this wire; magnetic coupling was indeed possible and important.

Even if inductive and capacitive interactions could be separated only in ideal, experimentally controllable geometries (this limitation is not obvious), then this ability would greatly simplify the design and understanding of experiments. When considering lumped element equivalent circuits of an experimental configuration, it is much simpler to deal with resistors and capacitors rather than with resistors, capacitors, inductors, and transformers. If the lumped

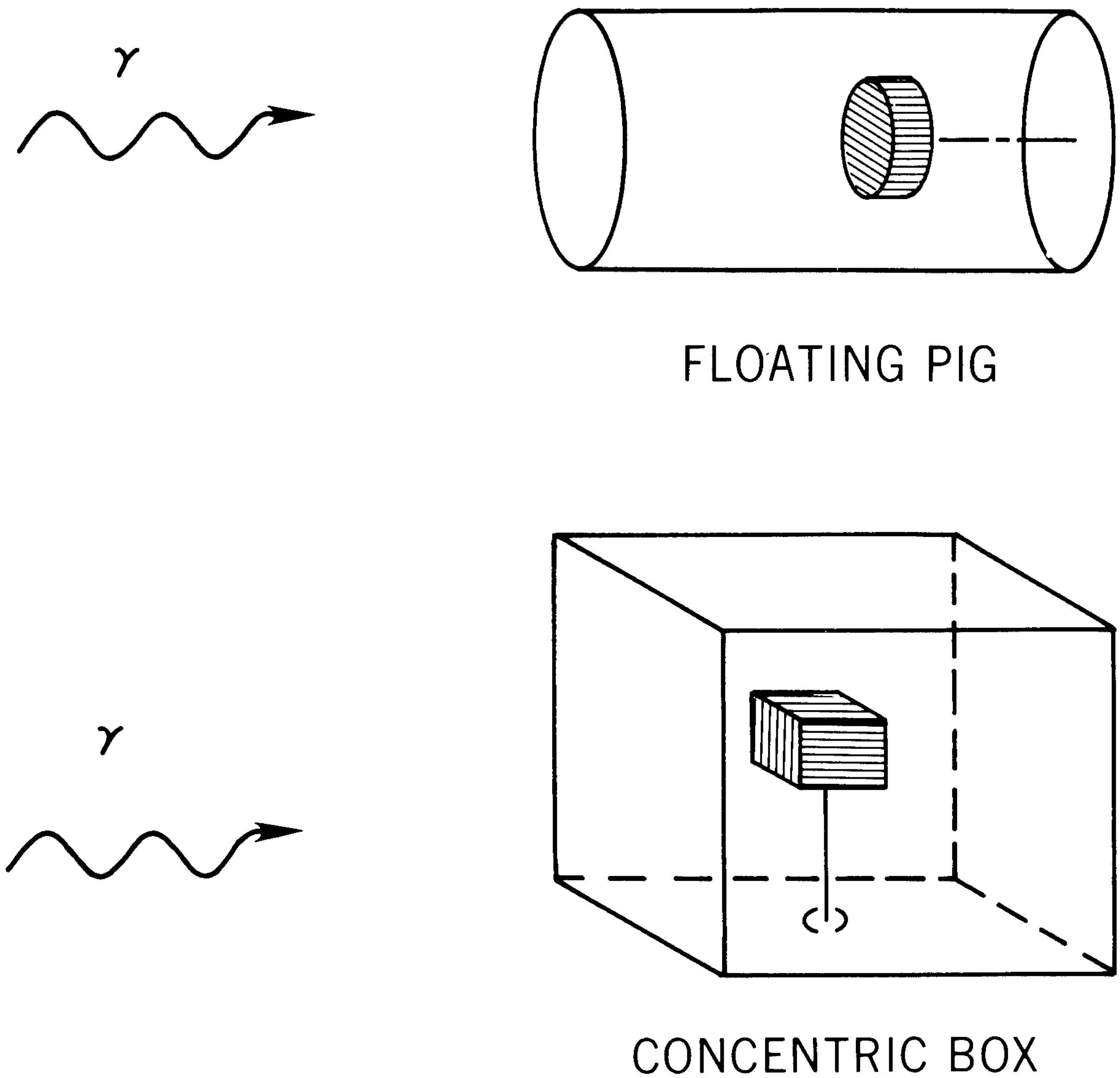

Figure 20. Inductive coupling.

parameters in the equivalent circuit are time varying and nonlinear, the difficulty with the coupling analysis is of even greater significance.

For example, Van Lint has suggested a simple approach to the determination of the voltages of the electrically free-floating gamma-thick absorber: (1) Insert different values of resistance between the gamma-thick absorber and the outer container. (2) Measure the current passing through the resistance between the absorber and the outer chamber when the concentric configuration is subjected to an AURORA pulse. Neglecting inductive effects, one can limit the equivalent circuit to a current source (the intercepted Compton current) feeding two parallel resistances, (1) the ionized gas, R_{gas}, and (2) the inserted resistance, R_{in}. In short, van Lint's suggestion can be used without complex computer codes. If the intercepted Compton current is given by $I_{Compton}$, then $V_{free} = R_{gas} I_{Compton}$ can be measured. It is easy to show by simple circuit theory that the current probe measures

$$I_{probe} = V_{free} / \left(R_{in} + R_{gas}\right). \tag{21}$$

One can measure I_{probe} and R_{in}. Therefore, a number of measurements should overdetermine R_{gas} and V_{free}. Actually, since R_{gas} is a time-varying function of the E-field, analysis is more complicated, but not as complicated as if one had to consider also magnetic effects.

3.7 Data Reduction

The following procedure is used to analyze the data taken during AURORA experiments: The oscilloscope pictures are digitized, and the digitized information is stored on a computer disk file. This information is read into a program which plots the data. The plot is compared with the oscilloscope picture, and any needed corrections are made to the digitized data. The digitized information is then read off the disk file by a computer code (developed at HDL) which (1) numerically transforms the digitized data into the frequency domain, (2) multiplies the frequency domain representation by the appropriate transfer function, (3) transforms this information back into the time domain, (4) multiplies the result by the appropriate sensor response and conversion factors, and (5) plots the resultant information. The plotted information represents the time histories of the actual fields, currents, etc., occurring at the sensor locations during the AURORA tests, not merely measured voltage at the oscilloscope. These plots are then compared with theoretical predictions of test results.

The transfer function used in the computer code is found experimentally. The sensor-cable-balun system used to make a measurement at the AURORA Facility is reassembled at the HDL Woodbridge Research Facility, and its frequency response is measured with a network analyzer to provide the transfer function.

3.8 Measurement of Electric Field Produced by Electrically Free Floating Pig

One of the reasons for performing the electrically free floating pig experiments is to investigate the possibility of charging a gamma-thick target and using it to enhance the E-field in a given volume. The behavior of the pig potential also might explain the behavior of a boundary layer as proposed by Longmire.[2] Another reason

[2]*C. L. Longmire, Direct Interaction Effect in EMP, Air Force Weapons Laboratory, EMP Interaction Note 69 (November 1973).*

for performing the series of pig experiments is that, unlike the pie-pan experiment, the potential of the pig is a function of time during and after the AURORA pulse. The potential on the pig and, therefore, on the boundary layer builds up during the first part of the AURORA gamma pulse. If the E-field measurements are being interpreted correctly, the boundary layer collapses after the AURORA pulse ceases. The collapse of the boundary layer in a bremsstrahlung free environment could be interpreted regarding the physics of the boundary layer.

For the measurements described in this report, an $\dot{E}$ sensor was used. Unfortunately, the results are confusing.

Assuming that the conductivity (σ) in equation (15) is 0, one obtains

$$E = \int_0^t dt' \left[\frac{1}{D}\frac{dV}{dt'} + \frac{1}{A\varepsilon_0 R} V(t')\right]$$

$$= \frac{1}{D}\int_0^t dt' \left[\frac{dV}{dt'} + \frac{D}{A\varepsilon_0 R} V(t')\right]$$

$$= \frac{1}{D}\int_0^t dt' \left[\frac{dV}{dt'} + \frac{V(t')}{CR}\right], \qquad (22)$$

where D is the distance between the sensor plates and E is the E-field between the plates. If CR > dt, one obtains (when the boundary layer can be ignored)

$$E = \frac{1}{D}\int_0^t dt' \frac{dV}{dt'}$$

$$= \frac{V}{D} . \qquad (23)$$

To obtain a situation in which $\sigma = 0$, a parallel-plate E-field sensor (fig. 21) was put behind a 22.9-cm-thick Pb pig as shown in figure 22. The pig served as a gamma shield. The measurements were carried out with two different gases in the tank, air and SF_6. The field sensor was positioned at several locations along the axis of the cylinder between the pig and the back wall. The voltage of the pig was determined by integrating the experimentally determined values of the E-field.

Some of the results of the experimental measurements are shown in figures 23 and 24. These two measurements were taken with the sensor shown in figure 21, 2.54 cm away from the back plate of the outer tank. This position is favorable because the E vectors would be perpendicular

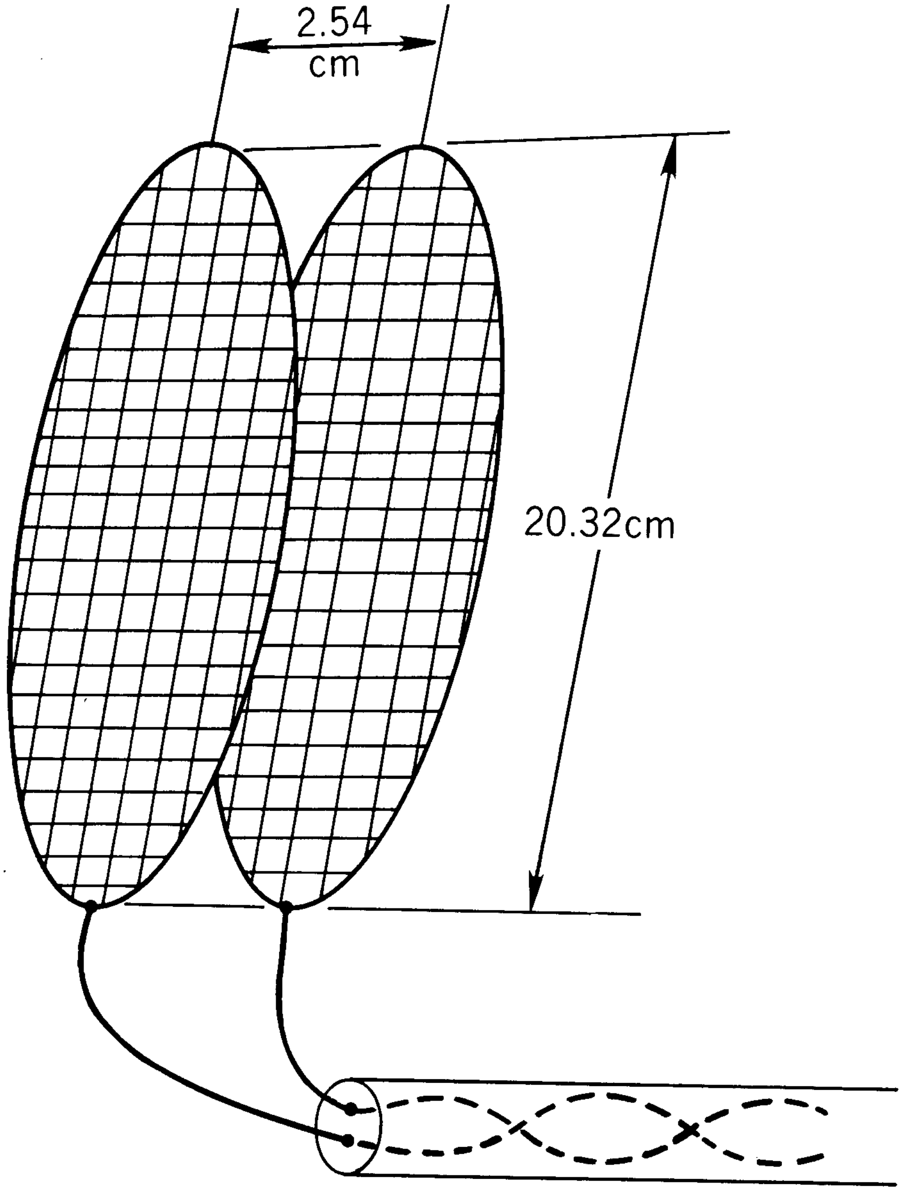

Figure 21. Whittaker $\dot{E}$ sensor.

to the back plate and, therefore, perpendicular to the E-field sensor. The integration of the $\dot{E}$ sensor measurements implies about 20,000 V between the pig and the outer cylinder.

In an effort to check our E-field measurements and also to investigate possible simulation techniques, the pig was subjected (fig. 25) to an AURORA gamma pulse while the pig was charged to (1) +2000 V and (2) -2000 V. The time constant of the power supply isolation was approximately 1 s. The results of these $\dot{E}$ and integrated $\dot{E}$ measurements are not consistent with an interpretation of the E-field

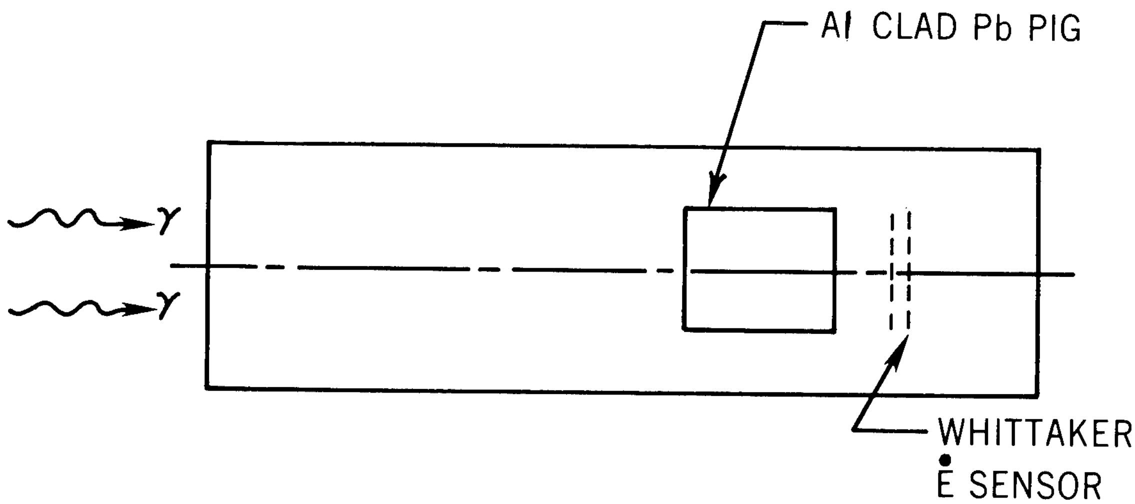

Figure 22. Floating pig.

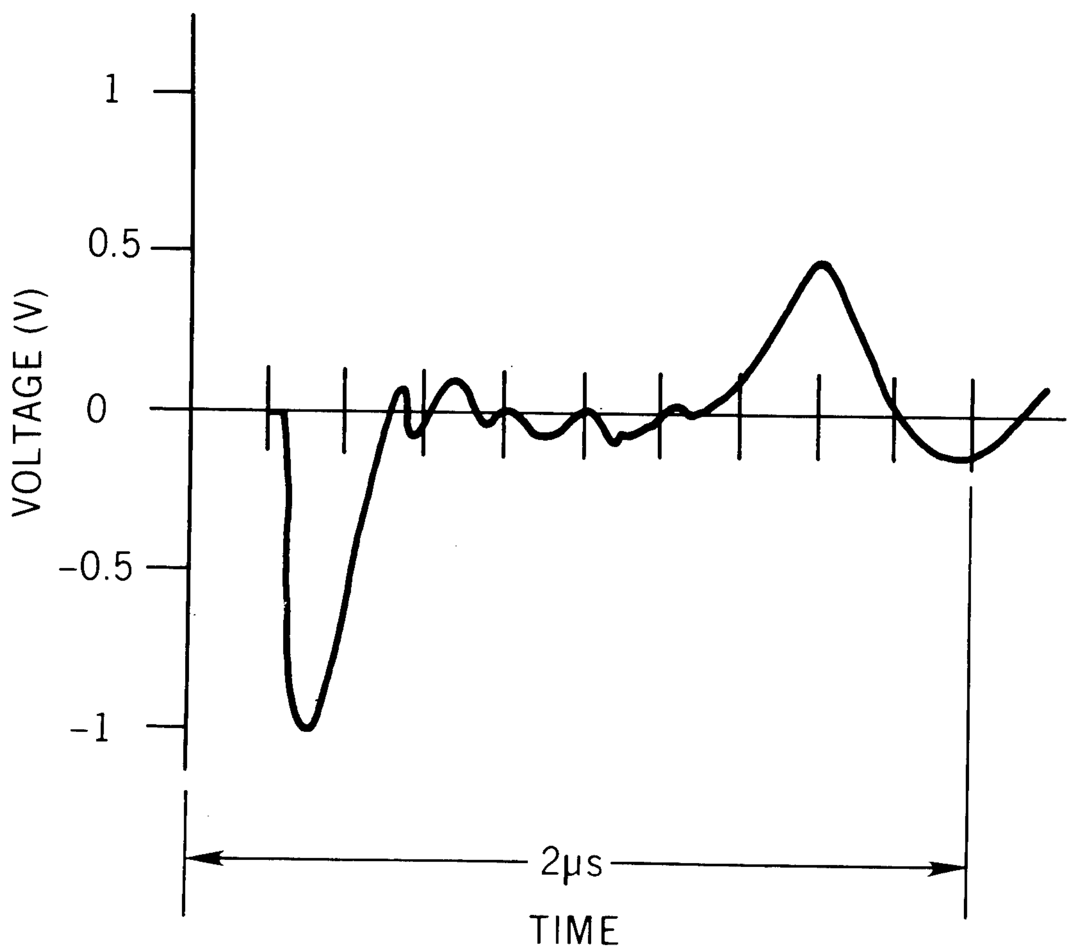

Figure 23. Output of $\dot{E}$ sensor (oscilloscope trace).

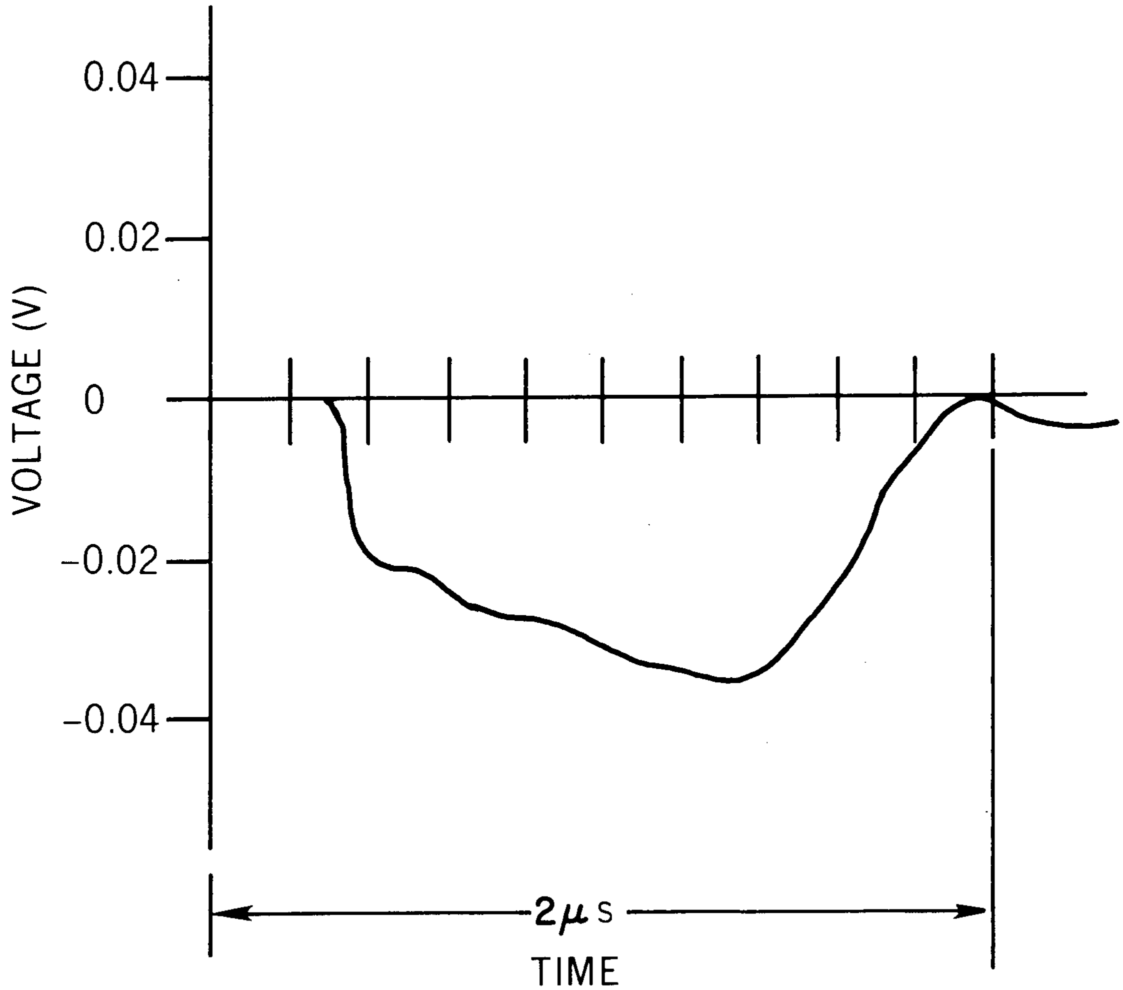

Figure 24. Integration of $\dot{E}$ sensor response.

sensor that neglects the effects of a boundary-layer formation at the grids of the Whittaker $\dot{E}$ sensor. The bias of ±2000 V has a much more significant effect than one would expect if the Compton current produced by AURORA bremsstrahlung were really charging the pig to 20,000 V. Depending on the sign of the bias, the 2000-V bias either increases or decreases the E-field measurements by about 50 percent. If the pig were really charged to 20,000 V, the 2000 V bias should not have more than a 10-percent effect. A possible explanation of this disparity is the formation of a boundary layer on the sensor plate. The boundary-layer effects may have been increased by the grid structure of the $\dot{E}$ sensor.

Although no definitive conclusions (based solely on any of these experiments) can be drawn concerning the feasibility of using a gamma-thick absorber as an E-field enhancer, the results lend insight

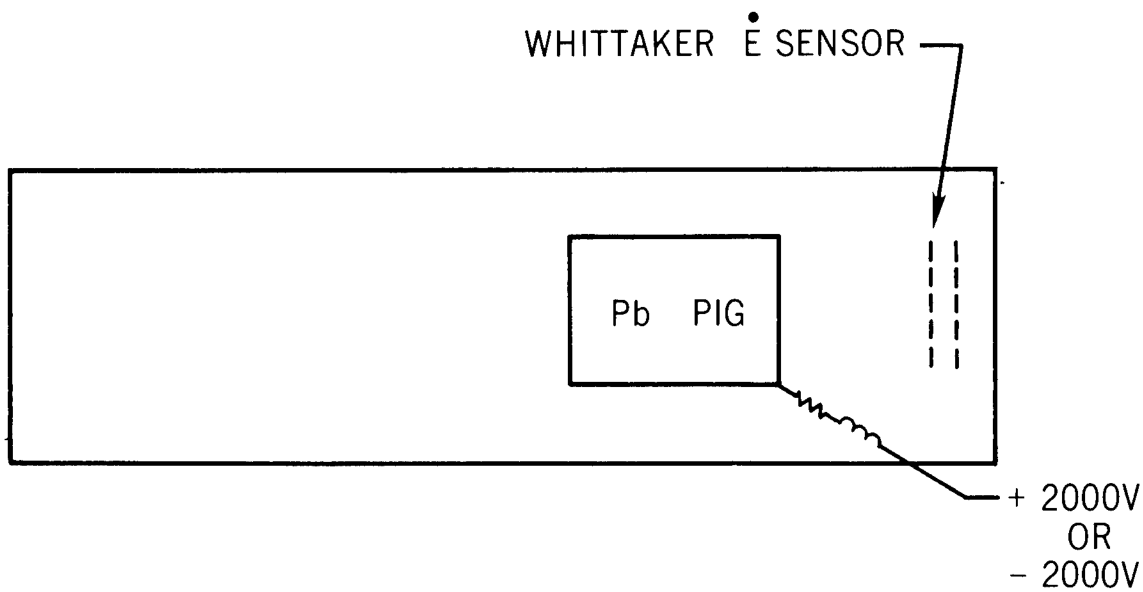

Figure 25. Charged pig.

into the phenomena of gamma-thick body charge collection and also indicate some of the potential engineering problems associated with using this as a method of simulation. These tentative indications are summarized below.

Because of the large conduction current term in equation (12), the significance of the $\dot{E}$ sensor is hard to understand when it is surrounded by ionized air produced by gamma rays in the open AURORA test cell. The straightforward integration of the $\dot{E}$ sensor yields rather large values of E. Boundary-layer effects also may be present.

To shield the $\dot{E}$ sensor, it was placed behind a pig, and thus the significance of the conduction between the grids was reduced. The results of the integrated E-fields in air implied a very large pig voltage.

The gas conductivity was reduced further when the tank was filled with SF_6. The resulting $\dot{E}$ measurements were large, as expected.

The pig was charged to 2000 V and subjected to the AURORA radiation. The results of the biasing appear to be inconsistent with the large E-fields implied by the measurements when the pig was not biased.

In light of the potential problems of boundary-layer interference in E-field measurements, a possible solution may be to use thin foils as the plates of the $\dot{E}$ sensor.

4. PLANS

In FY77, the major goals of TEMSEP to be fulfilled at HDL will continue the efforts of the study described in this report:

a. To develop adequate instrumentation to experimentally characterize the electromagnetic environment in the AURORA test cell.

b. To make the necessary measurements and perform theoretical calculations to fully and adequately characterize the electromagnetic environment in the AURORA test cell.

c. To develop an experimentally verified theoretical model for boundary-layer phenomena and determine the significance of such phenomena in tactical source-region situations of interest.

d. To theoretically determine the requirement for self-consistent interaction and coupling calculations for tactical source-region situations.

e. To develop an experimentally verified library of source-region coupling codes for tactical system applications.

f. To specify a technically feasible modification of the AURORA Facility for simulating worst-case source-region EMP environments of tactical interest. The simulation concept will be formulated in an attempt to accommodate both controlled diagonal experiments (oriented toward coupling code verification) and limited system or subsystem tests.

g. To perform state-of-the-art vulnerability estimates and, if necessary, make hardening recommendations for the AN/PRC-77 Radio Set and AN/TRC-145 Radio Terminal Set by using the existing EMP survivability criteria for tactical endoatmospheric threats.

LITERATURE CITED

(1) J. F. W. Dietz, G. Merkel, and D. Spohn, Radiation Induced Coupling to a Truncated Cylinder within a Cylinder, IEEE Trans. Nucl. Sci., NS-23 (December 1976).

(2) C. L. Longmire, Direct Interaction Effect in EMP, Air Force Weapons Laboratory, EMP Interaction Note 69 (November 1973).

(3) R. A. Perala et al, Coupling Calculations for the LANCE Missile System in a Tactical Nuclear Environment (U), Mission Research Corp. Report No. AMRC-IR-76457 (March 1976). (SECRET RESTRICTED DATA).

(4) R. A. Perala et al, Close-in Coupling Analysis of the AN/GRC-106 Radio System (U), Mission Research Corp. Report No. AMRC-IR-76458 (March 1976). (SECRET)

(5) Daniel L. Goodwin, The LANCE Electromagnetic Pulse (EMP) Assessment--Endoatmospheric Threat (U), Harry Diamond Laboratories TM-77-14 (October 1977). (CONFIDENTIAL)

(6) C. E. Baum, Radiation and Conductivity Constraints on the Design of a Dipole Electric Field Sensor, Air Force Weapons Laboratory EMP Sensor and Simulation Note 15 (June 1970).

(7) P. A. Trimmer, Transient Radiation Effects on Basic Triode Amplifiers, Harry Diamond Laboratories TR-1197 (April 1964).

DISTRIBUTION

DEFENSE DOCUMENTATION CENTER
CAMERON STATION, BUILDING 5
ALEXANDRIA, VA 22314
ATTN DDC-TCA (12 COPIES)

COMMANDER
USA RSCH & STD GP (EUR)
BOX 65
FPO NEW YORK 09510
ATTN LTC JAMES M. KENNEDY, JR.
CHIEF, PHYSICS & MATH BRANCH

COMMANDER
US ARMY MATERIEL DEVELOPMENT
& READINESS COMMAND
5001 EISENHOWER AVENUE
ALEXANDRIA, VA 22333
ATTN DRXAM-TL, HQ TECH LIBRARY

COMMANDER
US ARMY ARMAMENT MATERIEL
READINESS COMMAND
ROCK ISLAND ARSENAL
ROCK ISLAND, IL 61201
ATTN DRSAR-ASF, FUZE & MUNITIONS
SPT DIV

COMMANDER
USA MISSILE & MUNITIONS CENTER
& SCHOOL
REDSTONE ARSENAL, AL 35809
ATTN ATSK-CTD-F

DIRECTOR
ARMED FORCES RADIOBIOLOGY
RESEARCH INSTITUTE
DEFENSE NUCLEAR AGENCY
NATIONAL NAVAL MEDICAL CENTER
BETHESDA, MD 20014
ATTN RPC
ATTN TECHNICAL LIBRARY

ASSISTANT TO THE SECRETARY OF DEFENSE
ATOMIC ENERGY
DEPARTMENT OF DEFENSE
WASHINGTON, DC 20301
ATTN STAFF ASST (R&D)

DIRECTOR
DEFENSE ADVANCED RSCH PROJ AGENCY
ARCHITECT BUILDING
1400 WILSON BLVD.
ARLINGTON, VA 22209
ATTN TECHNICAL LIBRARY
ATTN AD/E&PS

DIRECTOR
DEFENSE CIVIL PREPAREDNESS AGENCY
ASSISTANT DIRECTOR FOR RESEARCH
WASHINGTON, DC 20301
ATTN TS(AED)
ATTN RE(EO)
ATTN ADMIN OFFICER
ATTN PO(SE)

DEFENSE COMMUNICATION ENGINEER CENTER
1860 WIEHLE AVENUE
RESTON, VA 22090
ATTN CODE R720, C. STANSBERRY
ATTN CODE R400
ATTN CODE R123, TECH LIB

DIRECTOR
DEFENSE COMMUNICATIONS AGENCY
WASHINGTON, DC 20305
ATTN CODE 930, MONTE I. BURGETT, FR
ATTN CCTC C312
ATTN CCTC/C672
ATTN CCTC C313
ATTN CODE 545

COMMANDER
DEFENSE ELECTRONIC SUPPLY CENTER
1507 WILMINGTON PIKE
DAYTON, OH 45401
ATTN ECS
ATTN ROSS V. DOUGHTY
ATTN EQ

DIRECTOR
DEFENSE INTELLIGENCE AGENCY
WASHINGTON, DC 20301
ATTN RDS-3A
ATTN DB-4C, EDWARD OFARRELL
ATTN RDS-3A4, POMPONIO PLAZA

DIRECTOR
DEFENSE NUCLEAR AGENCY
WASHINGTON, DC 20305
ATTN RATN
ATTN DDST
ATTN RAEV
ATTN TITL TECH LIBRARY
ATTN TISI ARCHIVES
ATTN STVL
ATTN RAAE

DIRECTOR OF DEFENSE RESEARCH
& ENGINEERING
DEPARTMENT OF DEFENSE
WASHINGTON, DC 20301
ATTN S&SS(OS)
ATTN G. BARSE

COMMANDER
FIELD COMMAND
DEFENSE NUCLEAR AGENCY
KIRTLAND AFB, NM 87115
ATTN FCPR
ATTN FCSM-F3/CDR SMITH
ATTN FCLMC

DIRECTOR
INTERSERVICE NUCLEAR WEAPONS SCHOOL
KIRTLAND AFB, NM 87115
ATTN DOCUMENT CONTROL

DIRECTOR
JOINT STRATEGIC TARGET
PLANNING STAFF, JCS
OFFUTT AFB
OMAHA, NB 68113
ATTN STINFO LIBRARY
ATTN JSAS
ATTN JLTW-2

CHIEF
LIVERMORE DIVISION, FIELD COMMAND DNA
LAWRENCE LIVERMORE LABORATORY
P.O. BOX 808
LIVERMORE, CA 94550
ATTN FCPRL

NATIONAL COMMUNICATIONS SYSTEM
OFFICE OF THE MANAGER
WASHINGTON, DC 20305
ATTN NCS-TS, CHARLES D. BODSON

DIRECTOR
NATIONAL SECURITY AGENCY
FT. GEORGE G. MEADE, MD 20755
ATTN O. O. VAN GUNTEN, R-425
ATTN TECHNICAL LIBRARY
ATTN R522
ATTN T1213
ATTN TDL
ATTN T412

OJCS/J-3
THE PENTAGON
WASHINGTON, DC 20301
ATTN J-3

PROJECT MANAGER
ARMY TACTICAL DATA SYSTEMS
US ARMY ELECTRONICS COMMAND
FORT MONMOUTH, NJ 07703
ATTN DRCPM-TDS-BSI

DIRECTOR
BMD ADVANCED TECH CTR
HUNTSVILLE OFFICE
PO BOX 1500
HUNTSVILLE, AL 35807
ATTN ATC-T

COMMANDER
BMD SYSTEM COMMAND
P.O. BOX 1500
HUNTSVILLE, AL 35807
ATTN BMDSC-AOLIB

COMMANDER
US ARMY ARMOR CENTER
FORT KNOX, KY 40121
ATTN TECHNICAL LIBRARY

DIRECTOR
US ARMY BALLISTIC RESEARCH LABS
ABERDEEN PROVING GROUND, MD 21005
ATTN DRSTE-EL
ATTN DRXBR-AM, W. R. VANANTWERP
ATTN DRDAR-BLE

COMMANDER
US ARMY COMM-ELEC ENGRG INSTAL AGY
FT HUACHUCA, AZ 85613
ATTN CCC-PRSO-S
ATTN CCC-CED-SES

COMMANDER
US ARMY COMMUNICATIONS COMMAND
FORT HUACHUCA, AZ 85613
ATTN CC-OPS-OS
ATTN CC-ENGR
ATTN CC-OPS-PD

COMMANDER
US ARMY COMMUNICATIONS COMMAND
COMBAT DEVELOPMENT DIVISION
FT. HUACHUCA, AZ 85613
ATTN ATSI-CD-MD

CHIEF
US ARMY COMMUNICATIONS SYSTEMS AGENCY
FORT MONMOUTH, NJ 07703
ATTN CCM-RD-T, CCM-AD-SV

COMMANDER
US ARMY ELECTRONICS COMMAND
FORT MONMOUTH, NJ 07703
ATTN DRSEL-CT-HDK, ABRAHAM E. COHEN
ATTN DRSEL-TL-MD, GERHART K. GAULE
ATTN DRSEL-GG-TD, W. R. WERK
ATTN DRSEL-TL-ME
ATTN DRSEL-NL-RO, R. BROWN

COMMANDER
US ARMY ELECTRONICS PROVING GROUND
FORT HUACHUCA, AZ 85613
ATTN STEEP-MT-M, GERALD W. DURBIN

DIVISION ENGINEER
US ARMY ENGINEER DIV HUNTSVILLE
P.O. BOX 1600, WEST STATION
HUNTSVILLE, AL 35807
ATTN HNDED-SR

US ARMY INTEL THREAT
ANALYSIS DETACHMENT
ROOM 2201, BLDG A
ARLINGTON HALL STATION
ARLINGTON, VA 22212
ATTN RM 2200, BLDG A

COMMANDER
US ARMY INTELLIGENCE & SEC COMMAND
ARLINGTON HALL STATION
4000 ARLINGTON BLVD
ARLINGTON, VA 22212
ATTN TECHNICAL LIBRARY
ATTN TECH INFO FAC

DIRECTOR
US ARMY MATERIEL SYS
ANALYSIS ACTIVITY
ABERDEEN PROVING GROUND, MD 21005
ATTN DRXSY-CC
ATTN DRXSY-PO

COMMANDER
US ARMY MISSILE RES & DEV COMMAND
REDSTONE ARSENAL, AL 35809
ATTN DRDMI-EAA
ATTN DRDMI-TBD
ATTN DRCPM-PE-EA, WALLACE O. WAGNER
ATTN DRCPM-PE-EG, WILLIAM B. JOHNSON

COMMANDER
US ARMY MISSILE MATERIEL
READINESS COMMAND
REDSTONE ARSENAL, AL 35809
ATTN DRCPM-LCEX, HOWARD H. HENRIKSEN
ATTN DRSMI-TRA, FAISON P. GIBSON

COMMANDER
US ARMY TANK AUTOMOTIVE COMMAND
WARREN, MI 48090
ATTN DRCPM-GCM-SW, LYLE A. WOLCOTT

COMMANDER
US ARMY TEST AND EVALUATION COMMAND
ABERDEEN PROVING GROUND, MD 21005
ATTN DRSTE-FA

COMMANDER
US ARMY TRAINING AND DOCTRINE COMMAND
FORT MONROE, VA 23651
ATTN ATORI-OP-SW

PROJECT OFFICER
US ARMY TAC COMM SYSTEMS
US ARMY ELECTRONICS COMMAND
FT MONMOUTH, NJ 07703
ATTN DRCPM-ATC

COMMANDER
WHITE SANDS MISSILE RANGE
WHITE SANDS MISSILE RANGE, NM 88002
ATTN D. E. MILLER
ATTN TE-AN, MR. OKUMA

CHIEF OF NAVAL RESEARCH
DEPARTMENT OF THE NAVY
ARLINGTON, VA 22217
ATTN CODE 464, R. GRACEN JOINER
ATTN CODE 427

OFFICER-IN-CHARGE
CIVIL ENGINEERING LABORATORY
NAVAL CONSTRUCTION BATTALION CENTER
PORT HUENEME, CA 93041
ATTN TECHNICAL LIBRARY

COMMANDER
NAVAL AIR SYSTEMS COMMAND
HEADQUARTERS
WASHINGTON, DC 21360
ATTN AIR-350F

COMMANDER
NAVAL ELECTRONIC SYSTEMS COMMAND
HEADQUARTERS
WASHINGTON, DC 20360
ATTN PME-117-215

COMMANDER
NAVAL OCEAN SYSTEMS CENTER
SAN DIEGO, CA 92152
ATTN CODE 812, S. W. LICHTMAN
ATTN CODE 015, C. FLETCHER
ATTN RESEARCH LIBRARY

SUPERINTENDENT (CODE 1424)
NAVAL POSTGRADUATE SCHOOL
MONTEREY, CA 93940
ATTN CODE 1424

COMMANDING OFFICER
NAVAL ORDNANCE STATION
INDIAN HEAD, MD 20640
ATTN STANDARDIZATION DEPT

DIRECTOR
NAVAL RESEARCH LABORATORY
WASHINGTON, DC 20375
ATTN CODE 4104, EMANUAL L. BRANCATO
ATTN CODE 2627, DORIS R. FOLEN
ATTN CODE 7701, JACK D. BROWN
ATTN CODE 7750
ATTN CODE 6624
ATTN CODE 6623, RICHARD L. STATLER

COMMANDER
NAVAL SHIP ENGINEERING CENTER
DEPARTMENT OF THE NAVY
WASHINGTON, DC 20362
(HYATTSVILLE)
ATTN CODE 6174D2, EDWARD F. DUFFY

COMMANDER
NAVAL SURFACE WEAPONS CENTER
WHITE OAK, SILVER SPRING, MD 20910
ATTN CODE 431, EDWIN R. RATHBURN
ATTN L. LIBELLO, CODE WR43
ATTN CODE WA51RH, RM 130-108

COMMANDER
NAVAL WEAPONS CENTER
CHINA LAKE, CA 93555
ATTN CODE 533, TECH LIB

DIRECTOR
STRATEGIC SYSTEMS PROJECT OFFICE
NAVY DEPARTMENT
WASHINGTON, DC 20376
ATTN NSP-2431, GERALD W. HOSKINS
ATTN NSP-230, DAVID GOLD
ATTN NSP-43, TECH LIB
ATTN NSP-27334
ATTN SP 2701, JOHN W. PITSENBERGER
ATTN NSP-2342, RICHARD L. COLEMAN

COMMANDER
US NAVAL COASTAL SYSTEMS LABORATORY
PANAMA CITY, FL 32401
ATTN TECH LIB

COMMANDER
ADC/DE
ENT AFB, CO 80912
ATTN DEEDS, JOSEPH C. BRANNAN

AF WEAPONS LABORATORY, AFSC
KIRTLAND AFB, NM 87117
ATTN NT, CARL E. BAUM
ATTN SUL
ATTN ELA, J. P. CASTILLO
ATTN NTS
ATTN SAB
ATTN ELXT
ATTN NT
ATTN CA
ATTN NTN
ATTN ELP

AFTAC
PATRICK AFB, FL 32925
ATTN TFS, MAJ MARION F. SCHNEIDER
ATTN TFE

COMMANDER
AIR UNIVERSITY
MAXWELL AFB, AL 36112
ATTN AUL/LSE-70-250

COMMANDER
ASD
WPAFB, OH 45433
ATTN ENFTV

HEADQUARTERS
ELECTRONIC SYSTEMS DIVISION/YS
HANSCOM AFB, MA 01731
ATTN YSEV

COMMANDER
FOREIGN TECHNOLOGY DIVISION, AFSC
WRIGHT-PATTERSON AFB, OH 45433
ATTN NICD LIBRARY
ATTN ETD, B. L. BALLARD

COMMANDER
OGDEN AIR LOGISTICS CENTER
HILL AFB, UT 84401
ATTN OO-ALC/MMETH, P. W. BERTHEL
ATTN MAJ RONALD BLACKBURN
ATTN MMEDO, LEO KIDMAN

COMMANDER
ROME AIR DEVELOPMENT CENTER, AFSC
GRIFFISS AFB, NY 13440
ATTN TSLD

COMMANDER
SACRAMENTO AIR LOGISTICS CENTER
MCCLELLAN AFB, CA 95652
ATTN MMSREM, F. R. SPEAR
ATTN MMARA, J. D. DUGAN
ATTN MMEAE, C. E. HOWARD
ATTN MMCRS, H. A. PELMASTRO
ATTN MMIRA, J. W. DEMES

SAMSO/IN
POST OFFICE BOX 92960
WORLDWAY POSTAL CENTER
LOS ANGELES, CA 90009
(INTELLIGENCE)
ATTN IND, I. J. JUDY

SAMSO/MN
NORTON AFB, CA 92409
(MINUTEMAN)
ATTN MNNH, MAJ M. BARAN
ATTN MNNH, CAPT R. I. LAWRENCE

SAMSO/SK
POST OFFICE BOX 92960
WORLDWAY POSTAL CENTER
LOS ANGELES, CA 90009
(SPACE COMM SYSTEMS)
ATTN SKF

SAMSO/YA
POST OFFICE BOX 92960
WORLDWAY POSTAL CENTER
LOS ANGELES, CA 90009
ATTN YAPC

COMMANDER IN CHIEF
STRATEGIC AIR COMMAND
OFFUTT AFB, NB 68113
ATTN NRI-STINFO LIBRARY
ATTN XPFS, MAJ BRIAN STEPHAN
ATTN DEL
ATTN JPST
ATTN JLTW
ATTN GARNET E. MATZKE

UNIVERSITY OF CALIFORNIA
LAWRENCE LIVERMORE LABORATORY
P.O. BOX 808
LIVERMORE, CA 94550
ATTN TERRY R. DONICH, L-96
ATTN HANS KRUGER, L-96
ATTN LIBRARIAN
ATTN WILLIAM J. HOGAN, L-389
ATTN DONALD J. MEEKER, L-545

LOS ALAMOS SCIENTIFIC LABORATORY
P.O. BOX 1663
LOS ALAMOS, NM 87545
ATTN DOC CON FOR CLARENCE BENTON
ATTN DOC CON FOR JOHN S. MALIK

SANDIA LABORATORIES
PO BOX 5800
ALBUQUERQUE, NM 87115
ATTN DOC CON FOR ORD 9353, R. L. PARKER
ATTN DOC CON FOR ELMER F. HARTMAN
ATTN C. N. VITTITOE, 5231

US ENERGY RSCH & DEV ADMIN
ALBUQUERQUE OPERATIONS OFFICE
P.O. BOX 5400
ALBUQUERQUE, NM 87115
ATTN OPERATIONAL SAFETY DIV
ATTN DOC CON FOR TECH LIBRARY

CENTRAL INTELLIGENCE AGENCY
ATTN: RD/SI, RM 5G48 HQ BLDG
WASHINGTON, DC 20505
ATTN OSI/NED/NWB

ADMINISTRATOR
DEFENSE ELECTRIC POWER ADMIN
DEPARTMENT OF THE INTERIOR
INTERIOR SOUTH BLDG, 312
WASHINGTON, DC 20240
ATTN L. O'NEILL

DEPARTMENT OF TRANSPORTATION
FEDERAL AVIATION ADMINISTRATION
HEADQUARTERS SEC DIV, ASE-300
800 INDEPENDENCE AVENUE, SW
WASHINGTON, DC 20591
ATTN SEC DIV ASE-300

NATIONAL OCEANIC & ATMOSPHERIC ADMIN
ENVIRONMENTAL RESEARCH LABORATORIES
DEPARTMENT OF COMMERCE
BOULDER, CO 80302
ATTN GLENN JEAN

AEROSPACE CORPORATION
PO BOX 92957
LOS ANGELES, CA 90009
ATTN C. B. PEARLSTON
ATTN IRVING M. GARFUNKEL
ATTN JULIAN REINHEIMER
ATTN LIBRARY
ATTN CHARLES GREENHOW

AGBABIAN ASSOCIATES
250 NORTH NASH STREET
EL SEGUNDO, CA 90245
ATTN LIBRARY

AVCO RESEARCH & SYSTEMS GROUP
201 LOWELL STREET
WILMINGTON, MA 01887
ATTN W. LEPSEVICH

BATTELLE MEMORIAL INSTITUTE
505 KING AVENUE
COLUMBUS, OH 43201
ATTN ROBERT M. BLAZEK
ATTN EUGENE R. LEACH

BDM CORPORATION, THE
7915 JONES BRANCH DRIVE
MCLEAN, VA 22101
ATTN TECHNICAL LIBRARY

BDM CORPORATION, THE
P.O. BOX 9274
ALBUQUERQUE INTERNATIONAL
ALBUQUERQUE, NM 87119
ATTN TECH LIB

BENDIX CORPORATION, THE
NAVIGATION AND CONTROL GROUP
TETERBORO, NJ 07608
ATTN DEPT 6401

BOEING COMPANY, THE
P.O. BOX 3707
SEATTLE, WA 98124
ATTN D. E. ISBELL
ATTN HOWARD W. WICKLEIN, MS 17-11
ATTN DAVID KEMLE
ATTN KENT TECH LIB
ATTN B. C. HANRAHAN

BOOZ-ALLEN AND HAMILTON, INC.
106 APPLE STREET
TINTON FALLS, NJ 07724
ATTN RAYMOND J. CHRISNER
ATTN TECH LIB

BROWN ENGINEERING COMPANY, INC.
CUMMINGS RESEARCH PARK
HUNTSVILLE, AL 35807
ATTN FRED LEONARD

BURROUGHS CORPORATION
FEDERAL AND SPECIAL SYSTEMS GROUP
CENTRAL AVE AND ROUTE 252
P.O. BOX 517
PAOLI, PA 19301
ATTN ANGELO J. MAURIELLO

CALSPAN CORPORATION
P.O. BOX 235
BUFFALO, NY 14221
ATTN TECHNICAL LIBRARY

CHARLES STARK DRAPER LABORATORY INC
555 TECHNOLOGY SQUARE
CAMBRIDGE, MA 02139
ATTN TIC, MS 74
ATTN KENNETH FERTIG

CINCINNATI ELECTRONICS CORPORATION
2630 GLENDALE - MILFORD ROAD
CINCINNATI, OH 45241
ATTN LOIS HAMMOND

COMPUTER SCIENCES CORPORATION
P.O. BOX 530
6565 ARLINGTON BLVD
FALLS CHURCH, VA 22046
ATTN RAMONA BRIGGS

COMPUTER SCIENCES CORPORATION
201 LA VETA DRIVE, NE
ALBUQUERQUE, NM 87108
ATTN ALVIN SCHIFF

CONTROL DATA CORPORATION
P.O. BOX 0
MINNEAPOLIS, MN 55440
ATTN JACK MEEHAN

CUTLER-HAMMER, INC.
AIL DIVISION
COMAC ROAD
DEER PARK, NY 11729
ATTN EDWARD KARPEN

DIKEWOOD INDUSTRIES, THE
1009 BRADBURY DRIVE, SE
ALBUQUERQUE, NM 87106
ATTN TECH LIB
ATTN L. WAYNE DAVIS

E-SYSTEMS INCORPORATED
ECI DIVISION
1501 DIVISION
1501 72ND STREET NORTH
ST PETERSBURG, FL 33733
ATTN RAYMOND D. FRANK

E-SYSTEMS, INC.
GREENVILLE DIVISION
P.O. BOX 1056
GREENVILLE, TX 75401
ATTN JOLETA MOORE

EFFECTS TECHNOLOGY, INC.
5383 HOLLISTER AVENUE
SANTA BARBARA, CA 93111
ATTN S. CLOW

EG&G, INC.
ALBUQUERQUE DIVISION
PO BOX 10218
ALBUQUERQUE, NM 87114
ATTN C. GILES

FAIRCHILD CAMERA AND INSTRUMENT CORP
464 ELLIS STREET
MOUNTAIN VIEW, CA 94040
ATTN SEC DEPT FOR 2-233,
DAVID K. MYERS

FORD AEROSPACE & COMMUNICATIONS CORP
3939 FABIAN WAY
PALO ALTO, CA 94303
ATTN LIBRARY
ATTN J. T. MATTINGLEY, MS X22
ATTN DONALD R. MCMORROW MS G30

FORD AEROSPACE & COMMUNICATIONS OPERATIONS
FORD & JAMBOREE ROADS
NEWPORT BEACH, CA 92663
ATTN KEN C. ATTINGER
ATTN E. R. PONCELET, JR.

FRANKLIN INSTITUTE, THE
20TH STREET AND PARKWAY
PHILADELPHIA, PA 19103
ATTN RAMIE H. THOMPSON

GENERAL DYNAMICS CORP
CONVAIR DIVISION
P.O. BOX 80847
SAN DIEGO, CA 92138
ATTN RSCH LIB

GENERAL DYNAMICS CORP
ELECTRONICS DIVISION
P.O. BOX 81127
SAN DIEGO, CA 92138
ATTN RSCH LIB

GENERAL ELECTRIC COMPANY
ORDNANCE SYSTEMS
100 PLASTICS AVENUE
PITTSFIELD, MA 01201
ATTN JOSEPH J. REIDL

GENERAL ELECTRIC COMPANY
TEMPO-CENTER FOR ADVANCED STUDIES
816 STATE STREET (PO DRAWER QQ)
SANTA BARBARA, CA 93102
ATTN DASIAC
ATTN ROYDEN R. RUTHERFORD
ATTN WILLIAM MCNAMERA

GENERAL ELECTRIC COMPANY
AEROSPACE ELECTRONICS SYSTEMS
FRENCH ROAD
UTICA, NY 13503
ATTN CHARLES M. HEWISON, DROP 624

GENERAL ELECTRIC COMPANY-TEMPO
ATTN: DASIAC
C/O DEFENSE NUCLEAR AGENCY
WASHINGTON, DC 20305
ATTN WILLIAM ALFONTE
ATTN ED ARNOLD

GENERAL RESEARCH CORPORATION
P.O. BOX 3587
SANTA BARBARA, CA 93105
ATTN TECH INFO OFFICE

GEORGIA INSTITUTE OF TECHNOLOGY
GEORGIA TECH RESEARCH INSTITUTE
ATLANTA, GA 30332
ATTN R. CURRY

GEORGIA INSTITUTE OF TECHNOLOGY
OFFICE OF CONTRACT ADMINISTRATION
ATTN: RSCH SECURITY COORDINATOR
ATLANTA, GA 30332
ATTN RES & SEC COORD FOR HUGH DENNY

GRUMMAN AEROSPACE CORPORATION
SOUTH OYSTER BAY ROAD
BETHPAGE, NY 11714
ATTN L-01 35

GTE SYLVANIA, INC.
ELECTRONICS SYSTEMS GRP-EASTERN DIV
77 A STREET
NEEDHAM, MA 02194
ATTN CHARLES A. THORNHILL, LIBRARIAN
ATTN LEONARD L. BLAISDELL

GTE SYLVANIA, INC.
189 B STREET
NEEDHAM HEIGHTS, MA 02194
ATTN CHARLES H. RAMSBOTTOM
ATTN DAVID P. FLOOD
ATTN COMM SYST DIV, EMIL P. MOTCHOK
ATTN H & V GROUP, MARIO A. NUREFORA
ATTN J. A. WALDRON

HARRIS CORPORATION
HARRIS SEMICONDUCTOR DIVISION
P.O. BOX 883
MELBOURNE, FL 32901
ATTN V. PRES & MGR PRGMS DIV

HONEYWELL INCORPORATED
AVIONICS DIVISION
2600 TIDGEWAY PARKWAY
MINNEAPOLIS, MN 55413
ATTN RONALD R. JOHNSON, A1622
ATTN S&RC LIB

HONEYWELL INCORPORATED
AVIONICS DIVISION
13350 US HIGHWAY 19 NORTH
ST. PETERSBURG, FL 33733
ATTN W. E. STEWART
ATTN M.S. 725-5, STACEY H. GRAFF

HUGHES AIRCRAFT COMPANY
CENTINELLA AND TEALE
CULVER CITY, CA 90230
ATTN CTOC 6/E110
ATTN JOHN B. SINGLETARY, MS 6-D133

IIT RESEARCH INSTITUTE
ELECTROMAG COMPATABILITY ANAL CTR
NORTH SEVERN
ANNAPOLIS, MD 21402
ATTN ACOAT

IIT RESEARCH INSTITUTE
10 WEST 35TH STREET
CHICAGO, IL 60616
ATTN IRVING N. MINDEL
ATTN JACK E. BRIDGES

INSTITUTE FOR DEFENSE ANALYSES
400 ARMY-NAVY DRIVE
ARLINGTON, VA 22202
ATTN TECH INFO OFC

INTL TEL & TELEGRAPH CORPORATION
500 WASHINGTON AVENUE
NUTLEY, NJ 07110
ATTN TECHNICAL LIBRARY

ION PHYSICS CORPORATION
SOUTH BEDFORD STREET
BURLINGTON, MA 01803
ATTN ROBERT D. EVANS

IRT CORPORATION
P.O. BOX 81087
SAN DIEGO, CA 92138
ATTN DENNIS SWIFT
ATTN C. B. WILLIAMS

JAYCOR
1401 CAMINO DEL MAR
DEL MAR, CA 92014
ATTN ERIC P. WENAAS
ATTN RALPH H. STAHL

JAYCOR
205 S WHITTING STREET, SUITE 500
ALEXANDRIA, VA 22304
ATTN TECH LIB

KAMAN SCIENCES CORPORATION
P.O. BOX 7463
COLORADO SPRINGS, CO 80933
ATTN ALBERT P. BRIDGES
ATTN W. FOSTER RICH
ATTN WALTER E. WARE
ATTN JERRY I. LUBELL
ATTN JOHN R. HOFFMAN
ATTN FRANK H. SHELTON

LITTON SYSTEMS, INC.
DATA SYSTEMS DIVISION
8000 WOODLEY AVENUE
VAN NUYS, CA 91409
ATTN M848-61
ATTN EMC GP

LITTON SYSTEMS, INC.
GUIDANCE & CONTROL SYSTEMS DIVISION
5500 CANOGA AVENUE
WOODLAND HILLS, CA 91364
ATTN JOE MOYER

LITTON SYSTEMS, INC.
AMECOM DIVISION
5115 CALVERT ROAD
COLLEGE PARK, MD 20740
ATTN J. SKAGGS

LOCKHEED MISSILES AND SPACE
COMPANY, INC.
P.O. BOX 504
SUNNYVALE, CA 94088
ATTN DEPT 85-85, SAMUEL I. TAIMUTY
ATTN G. F. HEATH, D/81-14
ATTN EDWIN A. SMITH, DEPT 85-85
ATTN H. E. THAYN
ATTN L. ROSSI, DEPT 81-64
ATTN BENJAMIN T. KIMURA, DEPT 81-14
ATTN M. J. BERNSTEIN

LOCKHEED MISSILES AND SPACE CO INC
3251 HANOVER STREET
PALO ALTO, CA 94304
ATTN TECH INFO CTR, D/COLL

M.I.T. LINCOLN LABORATORY
P.O. BOX 73
LEXINGTON, MA 02173
ATTN LEONA LOUGHLIN, LIBRARIAN A-082

MARTIN MARIETTA AEROSPACE
ORLANDO DIVISION
P.O. BOX 5837
ORLANDO, FL 32805
ATTN MONA C. GRIFFITH, LIB MP-30

MAXWELL LABORATORIES, INC.
9244 BALBOA AVENUE
SAN DIEGO, CA 92123
ATTN A. W. TRAVELPIECE

MCDONNELL DOUGLAS CORPORATION
POST OFFICE BOX 516
ST. LOUIS, MO 63166
ATTN TOM ENDER

MCDONNELL DOUGLAS CORPORATION
5301 BOLSA AVENUE
HUNTINGTON BEACH, CA 92647
ATTN STANLEY SCHNEIDER
ATTN TECH LIBRARY SERVICES

MISSION RESEARCH CORPORATION
735 STATE STREET
SANTA BARBARA, CA 93101
ATTN WILLIAM C. HART
ATTN EMP GROUP

MISSION RESEARCH CORPORATION
P.O. BOX 8693, STATION C
ALBUQUERQUE, NM 87108
ATTN DAVID E. MEREWETHER
ATTN L. N. MCCORMICK

MISSION RESEARCH CORPORATION-SAN
DIEGO
P.O. BOX 1209
LA JOLLA, CA 92038
ATTN V. A. J. VAN LINT

MITRE CORPORATION, THE
P.O. BOX 208
BEDFORD, MA 01730
ATTN THEODORE JARVIS
ATTN M. E. FITZGERALD

NORTHROP CORPORATION
NORTHROP RESEARCH AND
TECHNOLOGY CENTER
3401 WEST BROADWAY
HAWTHORNE, CA 90250
ATTN LIBRARY

NORTHROP CORPORATION
ELECTRONIC DIVISION
2301 WEST 120TH STREET
HAWTHORNE, CA 90250
ATTN VINCENT R. DEMARTINO
ATTN TECH LIB
ATTN LEW SMITH
ATTN RAD EFFECTS GRP, B. AHLPORT

PHYSICS INTERNATIONAL COMPANY
2700 MERCED STREET
SAN LEANDRO, CA 94577
ATTN DOC CON

PULSAR ASSOCIATES, INC.
7911 HERSCHEL AVENUE
LA JOLLA, CA 92037
ATTN V. FARGO
ATTN SECURITY

R & D ASSOCIATES
PO BOX 9695
MARINA DEL REY, CA 90291
ATTN S. CLAY ROGERS
ATTN LEONARD SCHLESSINGER
ATTN CHARLES MO
ATTN RICHARD R. SCHAEFER
ATTN DOC CON

RAND CORPORATION, THE
1700 MAIN STREET
SANTA MONICA, CA 90406
ATTN LIB-D
ATTN CULLEN CRAIN

RAY PROOF CORPORATION
P.O. BOX 60
NORWICK, CT 06856
ATTN E. S. KESNER

RAYTHEON COMPANY
HARTWELL ROAD
BEDFORD, MA 01730
ATTN GAJANAN H. JOSHI,
RADAR SYS LAB

RAYTHEON COMPANY
528 BOSTON POST ROAD
SUDBURY, MA 01776
ATTN HAROLD L. FLESCHER

RCA CORPORATION
GOVERNMENT SYSTEMS DIVISION
ASTRO ELECTRONICS
PO BOX 800, LOCUST CORNER
EAST WINDSOR TOWNSHIP
PRINCETON, NJ 08540
ATTN GEORGE J. BRUCKER

RCA CORPORATION
CAMDEN COMPLEX
FRONT & COOPER STREETS
CAMDEN, NJ 08012
ATTN R. W. ROSTROM, 13-5-2
ATTN OLIVE WHITEHEAD

ROCKWELL INTERNATIONAL CORPORATION
P.O. BOX 3105
ANAHEIM, CA 92803
ATTN J. L. MONROE, DEPT 243-027, DIV 031
ATTN D/243-068, 031-CA31
ATTN V. J. MICHEL

ROCKWELL INTERNATIONAL CORPORATION
SPACE DIVISION
12214 SOUTH LAKEWOOD BOULEVARD
DOWNEY, CA 90241
ATTN B. E. WHITE

ROCKWELL INTERNATIONAL CORPORATION
5701 WEST IMPERIAL HIGHWAY
LOS ANGELES, CA 90009
ATTN B-1 DIV TIC (BAOB)

SCIENCE APPLICATIONS, INC.
P.O. BOX 277
BERKELEY, CA 94701
ATTN FREDERICK M. TESCHE

SCIENCE APPLICATIONS, INC.
PO BOX 2351
LA JOLLA, CA 92038
ATTN R. PARKINSON

SCIENCE APPLICATIONS, INC.
HUNTSVILLE DIVISION
2109 W. CLINTON AVENUE
SUITE 700
HUNTSVILLE, AL 35805
ATTN NOEL R. BYRN

SCIENCE APPLICATIONS, INC.
8400 WESTPARK DRIVE
MCLEAN, VA 22101
ATTN WILLIAM L. CHADSEY

SINGER COMPANY, THE
ATTN: SECURITY MANAGER
1150 MC BRIDE AVENUE
LITTLE FALLS, NJ 07424
ATTN TECH INFO CTR

SPERRY FLIGHT SYSTEMS DIVISION
SPERRY RAND CORPORATION
P.O. BOX 21111
PHOENIX, AZ 85036
ATTN D. ANDREW SCHOW

SPERRY RAND CORPORATION
SPERRY MICROWAVE ELECTRONICS
P.O. BOX 4648
CLEARWATER, FL 33518
ATTN MARGARET CORT

SPERRY RAND CORPORATION
SPERRY DIVISION
MARCUS AVENUE
GREAT NECK, NY 11020
ATTN TECH LIB

SPIRE CORPORATION
P.O. BOX D
PATRIOTS PARK
BEDFORD, MA 01730
ATTN ROGER G. LITTLE

SRI INTERNATIONAL
333 RAVENSWOOD AVENUE
MENLO PARK, CA 94025
ATTN GEORGE CARPENTER
ATTN ARTHUR LEE WHITSON

SRI INTERNATIONAL
306 WYNN DRIVE, N. W.
HUNTSVILLE, AL 35805
ATTN MR. HULLINGS

SYSTEMS, SCIENCE AND SOFTWARE, INC.
PO BOX 1620
LA JOLLA, CA 92038
ATTN ANDREW R. WILSON

TEXAS INSTRUMENTS, INC.
P.O. BOX 6015
DALLAS, TX 75222
ATTN TECH LIB
ATTN DONALD J. MANUS, MS 72

TEXAS TECH UNIVERSITY
P.O. BOX 5404 NORTH COLLEGE STATION
LUBBOCK, TX 79417
ATTN TRAVIS L. SIMPSON

TRW DEFENSE & SPACE SYS GROUP
ONE SPACE PARK
REDONDO BEACH, CA 90278
ATTN O. E. ADAMS, R1-1144
ATTN ROBERT M. WEBB, R1-2410
ATTN R. K. PLEBUCH, R1-2078
ATTN H. H. HOLLOWAY, R1-2036
ATTN L. R. MAGNOLIA

TRW SYSTEMS GROUP
P.O. BOX 368
CLEARFIELD, UT 84015
ATTN DONALD W. PUGSLEY

UNITED TECHNOLOGIES CORP
NORDEN DIVISION
HELEN STREET
NORWALK, CT 06851
ATTN TECH LIB

UNITED TECHNOLOGIES CORPORATION
HAMILTON STANDARD DIVISION
BRADLEY INTERNATIONAL AIRPORT
WINDSOR LOCKS, CT 06069
ATTN CHIEF ELEC DESIGN

VECTOR RESEARCH ASSOCIATES
735 STATE STREET
SANTA BARBARA, CA 93101
ATTN W. A. RADASKY

WESTINGHOUSE ELECTRIC CORPORATION
ADVANCED ENERGY SYSTEMS DIV
P.O. BOX 10864
PITTSBURGH, PA 15236
ATTN TECH LIB

HARRY DIAMOND LABORATORIES
ATTN DANIEL, CHARLES D., JR., MG, COMMANDING GENERAL (ERADCOM)
ATTN RAMSDEN, JOHN J., LTC, COMMANDER/ FLYER, I.N./LANDIS, P.E./ SOMMER, H./OSWALD, R. B.
ATTN CARTER, W.W., DR., TECHNICAL DIRECTOR/MARCUS, S.M.
ATTN KIMMEL, S., PAO
ATTN CHIEF, 0021
ATTN CHIEF, 0022
ATTN CHIEF, LAB 100
ATTN CHIEF, LAB 200
ATTN CHIEF, LAB 300
ATTN CHIEF, LAB 400
ATTN CHIEF, LAB 500
ATTN CHIEF, LAB 600
ATTN CHIEF, DIV 700
ATTN CHIEF, DIV 800
ATTN CHIEF, LAB 900
ATTN CHIEF, LAB 1000
ATTN RECORD COPY, BR 041
ATTN HDL LIBRARY (5 COPIES)
ATTN CHAIRMAN, EDITORIAL COMMITTEE
ATTN CHIEF, 047
ATTN TECH REPORTS, 013
ATTN PATENT LAW BRANCH, 071
ATTN GIDEP OFFICE, 741
ATTN LANHAM, C., 0021
ATTN CHIEF, 1010
ATTN CHIEF 1020
ATTN CHIEF 1030 (20 COPIES)
ATTN CHIEF 1040
ATTN CHIEF 1050
ATTN CHEIF 340
ATTN CHIEF, 210
ATTN CHIEF, 0024